High-pressure spectroscopy of deep states induced by electron irradiation in A^4B^6 semiconductors: (A Review)

N. B. Brandt and E. P. Skipetrov*

M. V. Lomonosov State University, 119899 Moscow, Russia
(Submitted January 19, 1996)
Fiz. Nizk. Temp. **22**, 870–891 (August 1996)

We present the results of experimental investigations of the energy spectrum of radiation-induced defects in electron-irradiated semiconductors based on A^4B^6 semiconductors $Pb_{1-x}Sn_xSe$ and $Pb_{1-x}Sn_xTe$, obtained by using the high-pressure spectroscopy of localized states. The main attention is paid to the experimental detection of states induced by irradiation, interpretation of qualitative effects associated with redistribution of electrons in irradiated crystals between allowed bands and radiation-induced states under pressure, construction and substantiation of models describing the reconstruction of the energy spectra of irradiated alloys by changing the tin concentration and pressure. Reconstruction of the density of states function in the resonant radiation-induced bands is discussed and the main parameters of the models of energy spectrum of electron-irradiated $Pb_{1-x}Sn_xSe$ and $Pb_{1-x}Sn_xTe$ are investigated. © *1996 American Institute of Physics.* [S1063-777X(96)00308-8]

PREFACE

Investigation of materials at low temperatures and under high pressures has always been an exciting subject since it opens the way to basically new information about the properties of matter. First attempts to work out a technique for such investigations were made as early as seventy years ago.[1] However, pressures beyond 100 bar were not attainable at that time. The effects observed under such pressures were quite weak and hence no significant progress was made as a result of these investigations.

The situation changed radically only in the middle of the forties when Lazarev and Kan[2] invented the famous "ice bomb" allowing the study of magnetic and electric properties of bulk samples under pressures up to 2000 bar over a wide temperature interval. The significance of this invention lies mainly in that the approach used here for attaining high pressures at low temperatures led to the development of a whole range of new techniques in which the pressure was created at high temperatures and the apparatus was then cooled to low temperatures. These techniques, which are based on the idea employed in Ref. 2, turned out to be most effective for low-temperature studies of a wide range of phenomena and were widely put into practice.

The present review, dedicated to Lazarev and Kan, the founders of low-temperature high-pressure research, is but a small illustration of the effectiveness of the technique of obtaining high pressures at low temperatures proposed by them.

1. INTRODUCTION

Narrow-gap semiconductors based on A^4B^6 compounds are extremely convenient objects for studying the energy spectrum of charge carriers under hydrostatic compression. First, the range of alloys based on A^4B^6 compounds ($Pb_{1-x}Sn_xSe$, $Pb_{1-x}Sn_xTe$, ...) makes it possible to vary the band gap over a wide range (right up to the band inversion point upon an appropriate variation of the tin concentration x) and parameters of free charge carriers. Second, depending on the composition of the alloys, these materials possess positive as well as negative pressure coefficients dE_g/dP describing the variation of the band gap. Finally, the introduction of impurities or radiation defects in these semiconductors results in radical modifications in the energy spectrum of charge carriers owing to the emergence of low-lying levels or bands of localized states in the forbidden gap or against the background of allowed states.

Under these conditions, hydrostatic pressure makes it possible to vary the forbidden gap smoothly over a wide range right up to transition to the gapless state and band inversion, thus making it possible to change the parameters of charge carriers in allowed bands, as well as the mutual arrangement of allowed bands and deep defect levels, and to induce redistribution of electrons between bands and localized states. Experimental high-pressure observation of fundamental effects like transition to gapless state and band inversion, variation of shape and connectedness of Fermi surface, metal–insulator and insulator–metal type transitions, etc. can serve as an effective tool for studying the energy spectrum of narrow-gap semiconductors and forms the basis of the spectroscopy of band and localized states under pressure. This technique was found to be useful, for example, for determining the parameters of the energy-momentum relation for charge carriers in undoped $Pb_{1-x}Sn_xSe$ alloys,[3,4] the position of the low-lying III group impurity levels in $Pb_{1-x}Sn_xTe$ alloys,[5,6] and radiation defect levels in electron-irradiated InSb,[7,8] etc.

Investigation of the structure of local impurity bands and other point defects in narrow-gap semiconductors is a promising trend in the technique employing spectroscopy under high pressure. Such a possibility emerges if localized states are resonant and overlap with the allowed band near its edge. The variation in the mutual arrangement of resonant and allowed bands under pressure leads to a redistribution of electrons between bands. In this case, we can obtain information about the resonant band width and hence reconstruct the

variation of density of states in it by studying the pressure dependence of electron concentration in the allowed band.

This review contains the results of investigations of the effect of electron irradiation and subsequent application of hydrostatic pressure on the electric and physical properties of $Pb_{1-x}Sn_xSe$ and $Pb_{1-x}Sn_xTe$ alloys, and an analysis of existing models of energy spectrum of radiation defects in electron-irradiated alloys describing the spectral rearrangement due to a change in composition and pressure. The basic parameters of models describing the energy spectrum of electron-irradiated alloys are determined by comparing the experimental results with the theoretical ones obtained with the help of the available models.

2. BAND STRUCTURE OF A^4B^6 SEMICONDUCTORS

Semiconducting alloys $Pb_{1-x}Sn_xTe$ and $Pb_{1-x}Sn_xSe(x<0.43)$ crystallize into an NaCl type lattice and are narrow-gap semiconductors with a direct gap at the L-point of the Brillouin zone.[9] The energy levels L_6^- and L_6^+ defining the edges of the conduction and valence bands approach upon an increase in tin concentration x in the alloy and suffer inversion at $x=x_i$ (at $T=4.2$ K, $x_i\simeq 0.15$ for $Pb_{1-x}Sn_xSe$ and $x_i\simeq 0.35$ for $Pb_{1-x}Sn_xTe$).

The band gap E_g for $Pb_{1-x}Sn_xTe(Se)$ is extremely sensitive to hydrostatic compression. The change in the band gap under pressure occurs almost linearly and is characterized by the pressure coefficients of gap variation $|dE_g/dP|\simeq 8.5$ meV/kbar for $Pb_{1-x}Sn_xSe$[9,10] and $|dE_g/dP|\simeq 7.4$ meV/kbar for $Pb_{1-x}Sn_xTe$,[9,11] whose magnitudes are practically independent of temperature and the alloy composition. The coefficient dE_g/dP is negative in alloys with a direct spectrum ($E_g>0$). Hence the band gap vanishes under a certain pressure and then begins to increase in magnitude. In alloys with an inverse spectrum ($E_g<0$), the coefficient dE_g/dP is positive and the band gap increases with pressure. Hence it can be assumed that the reconstruction of the energy spectrum under pressure is on the whole analogous to the reconstruction of the spectrum upon an increase in the tin concentration in the alloys.

A characteristic feature of the band structure of alloys is the existence of a group of six closely spaced energy bands at the point L of the Brillouin zone. Hence we must take into consideration the interaction of six bands at the point L while using the $\mathbf{k}\cdot\mathbf{p}$ method to calculate the structure of conduction and valence band edges in the vicinity of the extrema. However, since the separation from the conduction and valence band edges to distant bands on the energy scale is much larger than band gap, the influence of distant bands can be disregarded in the zeroth approximation. The energy-momentum relation in the two-band approximation has the form

$$E^2-\frac{E_g^2}{4}=E_\perp\frac{p_\perp^2}{2m_0}+E_\parallel\frac{p_\parallel^2}{2m_0}, \tag{1}$$

where E is the energy (measured from the middle of the band gap), E_g is the direct band gap at L, $E_\perp=2P_\perp^2/m_0$, $E_\parallel=2P_\parallel^2/m_0$, $P_\perp$ and $P_\parallel$ being the transverse and longitudinal matrix elements of the momentum operator characterizing the interaction between the valence and conduction bands.

Thus, for valence and conduction bands, the constant energy surfaces in the vicinity of points L have the form of ellipsoids of revolution with the major axis parallel to the directions of the type $\langle 111\rangle$, while the Fermi surface consists of four ellipsoidal surfaces with centers at points L. These surfaces are filled with electrons for n-type alloys and with holes for p-type alloys.

Dimmock[12] and Martinez[13] took into account the effect of distant bands at the point L in the $\mathbf{k}\cdot\mathbf{p}$ method. The interaction between the valence and conduction bands was considered precisely, while the interaction with distant bands was taken up to second and third orders, respectively, in the perturbation theory according to Levdin. Dimmock's energy-momentum relation has the form

$$\left(\frac{E_g}{2}+\frac{p_\perp^2}{2m_t^-}+\frac{p_\parallel^2}{2m_l^-}-E\right)\left(-\frac{E_g}{2}-\frac{p_\perp^2}{2m_t^+}-\frac{p_\parallel^2}{2m_l^+}-E\right)=E_\perp\frac{p_\perp^2}{2m_0}+E_\parallel\frac{p_\parallel^2}{2m_0}, \tag{2}$$

where $E_\perp$, $E_\parallel$ and $m_t^\pm$, $m_l^\pm$ are the model parameters taking into account the interaction of the valence and conduction bands with each other and with distant bands respectively.

According to Dimmock's energy-momentum relation, the electron and hole spectra are not mirror images in the general case, and the constant-energy surfaces in the conduction and valence bands are nonellipsoidal surfaces of revolution (the energy-momentum relation contains terms proportional to p^4) whose anisotropy coefficient depends on the energy E (number density of charge carriers) and the forbidden band width E_g (concentration of tin in the alloy and pressure).

Martinez also carried out a detailed theoretical analysis of the reconstruction of the energy spectrum of $Pb_{1-x}Sn_xSe$ alloys under uniform compression.[13] He assumed that the energy spectrum parameters depend only on the gap E_g and not on the manner in which this value was obtained (whether by changing the tin concentration in the alloy or the value of the applied pressure). In this respect, the results of calculations of the energy spectrum of $Pb_{1-x}Sn_xSe$ obtained by the six-band models proposed by Dimmock and Martinez are analogous, and practically identical up to the band gap $E_g\simeq -100$ meV, according to Martinez.

Dimmock's model is widely used at present for analyzing the experimental results obtained while studying the band structure of $Pb_{1-x}Sn_xSe(Te)$. Several sets of parameters proposed for this model make it possible to obtain a satisfactory agreement with the experimental data over a wide range of variation of concentration of tin and charge carriers.[4,14]

3. ENERGY SPECTRUM OF RADIATION DEFECTS IN ELECTRON-IRRADIATED A^4B^6 SEMICONDUCTORS

The effect of irradiation by fast particles on the energy spectrum of charge carriers in A^4B^6 semiconductors has been studied since the middle of the seventies. First investigations were devoted to the effect of low-temperature ($T_{rad} \leqslant 80$ K) and high-temperature ($T_{rad} \simeq 300$ K) electron irradiation on electrical and physical properties of the alloys ($Pb_{1-x}Sn_xTe$ and $Pb_{1-x}Sn_xSe$)[15,19] and were stimulated largely by the theoretical works of Parada and Pratt on the energy spectrum of simple intrinsic defects in PbTe (vacancies and interstitial atoms in metal and chalcogen sublattices).[20–22] According to their calculations, as well as later works by Hemstreet,[23,24] the energy levels of simple point defects in A^4B^6 belong to the category of low-lying levels and must be situated away from the forbidden band edges in conduction and valence bands against the background of allowed states. The only exception to this is the chalcogen vacancy whose energy levels may be close to the conduction band edge or even in the forbidden gap.

On the basis of the theoretical calculations, the experimental data were interpreted for a long time under the assumption that the defects emerging as a result of irradiation of crystals by fast particles are simple point defects similar to the defects in the initial unexposed crystals. The chalcogen vacancy was assumed to be the most important kind of defect. A whole range of publications was devoted to the attempts at a direct experimental observation of deep chalcogen vacancy levels in initial crystals and those irradiated by fast particles.

Considerable progress in these investigations was made following the publication of a series of works by Volkov and Pankratov,[25,26] as well as by Pankratov and Povarov,[27,28] in which a change in the position of the chalcogen vacancy level relative to the allowed band edges at L upon an increase in the tin concentration in alloys was predicted on the basis of analytic calculations of energy levels of simple defects in the alloys $Pb_{1-x}Sn_xTe$ and $Pb_{1-x}Sn_xSe$.

Investigation of alloys with different concentrations of tin and the application of pressure indeed led to the discovery of several deep defect levels in the forbidden band as well as against the background of allowed states of valence and conduction bands of irradiated alloys. However, it has now become clear that as in other more thoroughly investigated semiconductors (Ge, Si, A^3B^5 compounds), these levels are associated not with simple defects like vacancies and interstitial atoms in metal and chalcogen sublattices, but rather with more complicated defects like complexes including primary radiation defects.

In spite of the fact that the precise microscopic structure of such defects in A^4B^6 semiconductors is not known so far, the available experimental data allow us to construct models of energy spectrum of radiation defects in electron-irradiated $Pb_{1-x}Sn_xSe$ and $Pb_{1-x}Sn_xTe$ alloys of various compositions.

3.1. $Pb_{1-x}Sn_xSe$ alloys

These alloys have been studied quite extensively. A model of energy spectrum explaining the experimental results correctly over a wide range of tin concentration ($0 \leqslant x \leqslant 0.34$), i.e., practically over the entire range of existence of cubic phase of the alloys, has been proposed.[29,30] According to this model, electron irradiation leads to the emergence of two deep levels (localized state bands) E_t and E_{t1} in the energy spectrum of these alloys, which are associated with different types of radiation defects. The position of these levels relative to the energy band edges at L depends on the alloy composition (Fig. 1).

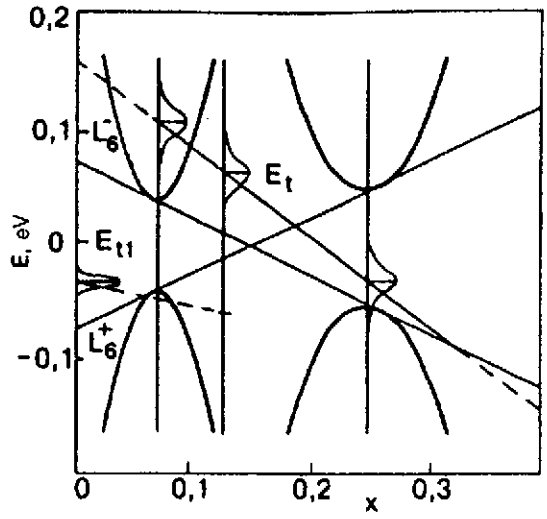

FIG. 1. Model of energy spectrum of electron-irradiated alloys $Pb_{1-x}Sn_xSe$.

The band E_t corresponding to radiation defects is not filled by electrons. Hence the states emerging as a result of irradiation may be neutral or exert an acceptor influence depending on their position relative to the Fermi level E_F. In alloys with a normal spectrum ($E_g > 0$), the local band is a resonant band and located against the background allowed states of the conduction band. Upon an increase in the tin concentration x, the local band descends on the energy scale and first falls in the forbidden gap and then in the valence band in alloys with inverse spectrum ($E_g < 0$). The most significant variations of parameters as a result of irradiation were observed for alloys with n-type conductivity and inverse spectrum, the middle of the E_t band in these alloys falling in the forbidden gap. The generation of defects as a result of irradiation in such alloys lowers the concentration of electrons in the conduction band and leads to a metal–insulator type transition as a result of electron flow from conduction band to the E_t band.

The radiation defect band E_{t1} is partially filled by electrons and possesses donor–acceptor properties. In PbSe and alloys with low tin concentration, the middle of the E_{t1} band lies in the forbidden gap near the top of the valence band. Hence an increase in the radiation flux (i.e., density of states in the E_{t1} band) results in a decrease in the electron concentration in n-type samples as a result of electron flow from the conduction band to the E_{t1} level, and a decrease in the hole concentration in p-type samples as a result of flow of electrons from the E_{t1} level to the valence band. Irrespective of the initial type of conductivity of alloys, a high radiation flux

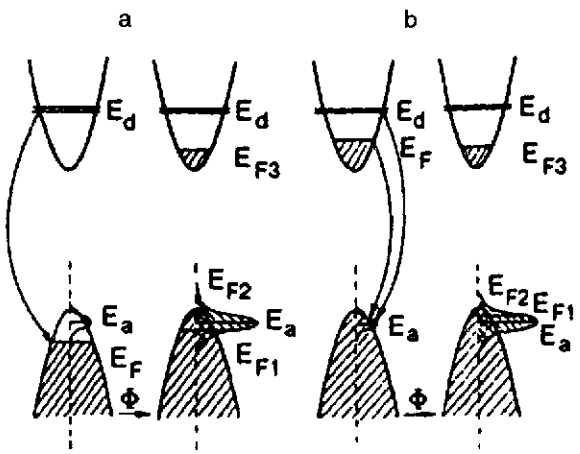

FIG. 2. Model of energy spectrum of electron-irradiated alloys $Pb_{1-x}Sn_xTe$. (a) p-type, (b) n-type.

leads to a transition to the insulating state in which the valence band is completely filled by electrons at low temperatures, the conduction band is completely free of electrons, and the E_{t1} band is partially filled by electrons. The occupancy of the E_{t1} band in the insulating state depends on the parameters of the initial crystal (charge carrier concentration) and the radiation flux.

3.2. $Pb_{1-x}Sn_xTe$ alloys

The $Pb_{1-x}Sn_xTe$ alloys have been studied much less intensively than $Pb_{1-x}Sn_xSe$. The effect of electron irradiation on the electrical and physical properties of the alloys was studied only in a narrow range of tin concentration ($0.135 \leqslant x \leqslant 0.22$), the majority of the results pertaining to the composition $x \approx 0.2$ which is most important from the practical point of view.[15-19,31,32]

On the whole, the experimental data obtained by different authors do not contradict one another and can be used to construct a unified model of energy spectrum of irradiated crystals with $x \approx 0.2$ (Fig. 2). According to this model, electron irradiation leads to the emergence of a resonant donor level E_d high in the conduction band, and an acceptor-type resonant states band E_a near the top of the valence band in the energy spectrum of the alloy. The change in the concentration of charge carriers due to irradiation is determined by the ratio of the donor and acceptor type defect generation rates, which apparently depends on the defect structure and type of conductivity of the initial crystals.

In crystals with p-type conductivity (Fig. 2a) for $dN_d/d\Phi < dN_a/d\Phi$, the hole concentration decreases with increasing radiation flux Φ as a result of flow of electrons from the donor level to the valence band, while the Fermi level tends to attain its limiting position. Depending on the ratio of the quantities $dN_d/d\Phi$ and $dN_a/d\Phi$, the resonant band width and position on the energy scale, the hole concentration may attain saturation (stabilization of the Fermi level E_{F1} in the valence band) or vanish (stabilization of the Fermi level E_{F2} in the forbidden band). For $dN_d/d\Phi > dN_a/d\Phi$, an increase in the radiation flux leads to a filling of the valence band and the resonant states band E_a and a decrease in hole concentration to zero. After this, the irradiated crystals are in insulating state over a finite interval (depending on the initial hole concentration in the sample) of radiation flux (right up to filling of the states at the tail of the density of resonance state bands lying in the forbidden gap). Finally, for maximum radiation flux, the Fermi level must be elevated to the conduction band (E_{F3}), and the electron concentration will increase until the Fermi level is stabilized by the donor level.

In crystals with n-type conductivity (Fig. 2b) for $dN_d/d\Phi < dN_a/d\Phi$, the electron concentration decreases with increasing radiation flux as a result of flow of electrons from the donor level and conduction band to the resonant band E_a, while the Fermi level tends to its limiting position. Depending on the relation between the quantities $dN_d/d\Phi$ and $dN_a/d\Phi$, the resonant band width and position on the energy scale, the electron concentration may vanish with increasing radiation flux (stabilization of the Fermi level E_{F2} in the forbidden band), or n–p-conversion may occur followed by stabilization of the Fermi level E_{F1} in the valence band. The version $dN_d/d\Phi > dN_a/d\Phi$ has not been detected experimentally so far, but it can be expected that the electron concentration may increase in this case right until the stabilization of the Fermi level by the E_d level.

Thus, irrespective of the type of conductivity of the initial crystals, irradiation by fast electrons leads to a stabilization of the Fermi level by the acceptor-type radiation defect band $E_a(dN_d/d\Phi < dN_a/d\Phi)$ or by the donor level $E_d(dN_d/d\Phi > dN_a/d\Phi)$.

No reliable data are available on the nature of reconstruction of the energy spectrum of radiation defects upon a change in the tin concentration in the alloys. However, the experimental results on proton irradiation of alloys with $0.17 \leqslant x \leqslant 0.26$ obtained in Refs. 33–35 show that the position of the resonant band E_a relative to the middle of the band gap does not vary significantly upon a change in the alloy composition. Hence the middle of the band E_a may turn out to be in the band gap upon a decrease in tin concentration ($x < 0.15$).

4. PRESSURE-INDUCED METAL–INSULATOR TRANSITION IN ELECTRON-IRRADIATED ALLOYS n-$Pb_{1-x}Sn_xSe$ ALLOYS WITH A DIRECT SPECTRUM

The model of energy spectrum of electron-irradiated $Pb_{1-x}Sn_xSe$ alloys (Fig. 1) assumes the possibility of an effective control over the properties of these alloys through electron irradiation and of observing a whole range of effects resulting from irradiation followed by a uniform compression of the irradiated alloys, viz., stabilization of Fermi level and attainment of limiting values of electrical and physical parameters under intensive electron irradiation, transitions to the insulating state under the effect of electron irradiation, uniform compression and a quantizing magnetic field. Among other things, the possibility of a considerable decrease in the charge carrier concentration in irradiated crystals right up to the insulating state transition as a result of the flow of charge carriers from the allowed states band to the radiation defect band E_t is realized upon compression of alloys with a normal spectrum ($E_g > 0$).

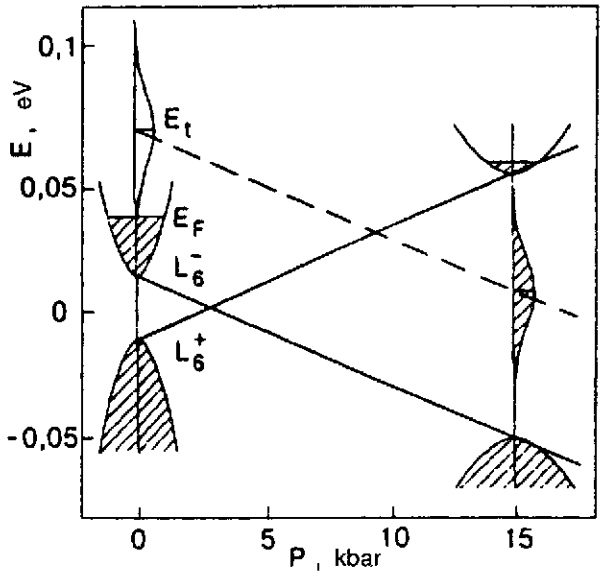

FIG. 3. Reconstruction of energy spectrum of the electron-irradiated alloy $Pb_{1-x}Sn_xSe$ ($x=0.125$)($N_t<n_0$) under pressure.

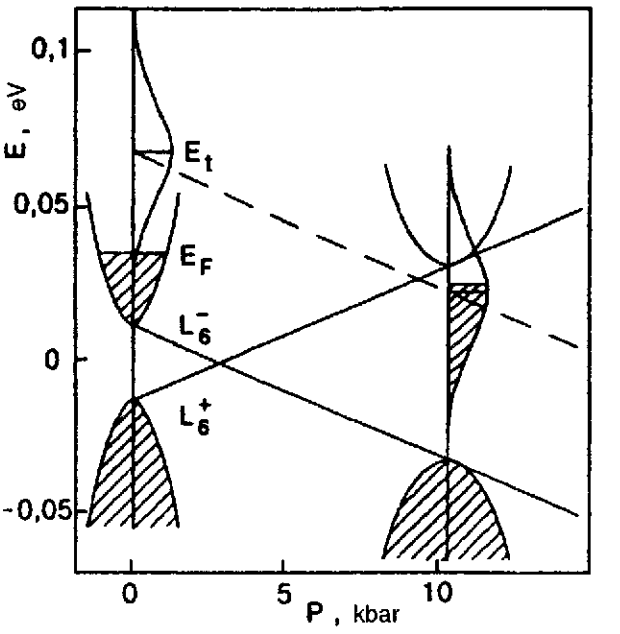

FIG. 4. Reconstruction of energy spectrum of electron-irradiated alloys $Pb_{1-x}Sn_xSe$ ($x=0.125$)($N_t>n_0$) under pressure.

The effect of uniform compression on electrical and physical properties of electron-irradiated n-type $Pb_{1-x}Sn_xSe$ ($x=0.07$, 0.125) alloys was studied in Refs. 29 and 36–42 in order to observe experimentally the pressure-induced metal–insulator transition, to determine the structure of the radiation defect band E_t and its position on the energy scale, and to obtain the diagram of reconstruction of the energy spectrum of the alloys under pressure.

4.1. Reconstruction of the energy spectrum under pressure

The hydrostatic compression of electron-irradiated alloys with a direct spectrum leads to a decrease in the electron concentration accompanied by stabilization of the Fermi level by the radiation defect band E_t. A model has been proposed for the reconstruction of the energy spectrum of irradiated alloys under pressure (Figs. 3 and 4). According to this model, a decrease in the electron concentration in irradiated alloys as a result of compression is a consequence of the redistribution of electrons between the conduction band and the radiation defect band.

The best agreement between the proposed model and the experimental results is attained by assuming that the separation between the middle of the localized states band E_t and the energy level L_6^- practically does not change with pressure. In this case, an increase in pressure leads first to a decrease in band gap at the point L, which results in a decrease in the effective mass of electrons and the density of states in the conduction band.[4,43] Hence, in spite of the unchanged separation between the bottom of the conduction band and the local band, the electron concentration decreases slowly as a result of a rise in the Fermi level and trapping of electrons by states at the tail of the local band density of states. After band inversion at the point L, the separation between the middle of the band E_t and the bottom of the conduction band L_6^+ decreases rapidly, resulting in a flow of electrons from the conduction band to the localized states band and a rapid decrease in the concentration of free electrons.

In the region of maximum compression, the middle of the local band E_t intersects the bottom of the conduction band and falls in the band gap. The nature of the pressure dependence of electrical and physical parameters of samples is determined by the relation between the total capacity of the localized states band N_t, which depends on the radiation flux, and the initial number density n_0 of electrons in the sample.

For $N_t<n_0$, the radiation defect band located in the band gap of the alloy is found to be completely filled by electrons (Fig. 3). Moreover, a part of electrons $n'=n_0-N_t$ remains in the conduction band. Hence, as the pressure increases, the electrical and physical parameters of samples of the first group tend to certain limiting values which depend on the residual number density of electrons n'.

For $N_t>n_0$, the radiation defect band is only partially filled by electrons in the maximum pressure region (Fig. 4). This means that with increasing pressure, the electrons are completely transferred from the conduction band to the localized states band. Under a certain critical pressure P^*, the electron concentration becomes equal to zero and the metal–insulator transition takes place.

The metal–insulator transition is accompanied by a sharp increase (about three orders of magnitude) in the resistivity and reversal of the sign of Hall constant (Fig. 5). With increasing radiation flux, the sign-reversal point R_X is displaced towards lower pressures, and the Hall constant is stabilized beyond the sign-reversal point at the level $R_X=40-100$ cm^3/C.

The positive sign of R_X in the insulating phase points towards a change in the type of majority carriers and is apparently due to the fact that the main conduction mechanism

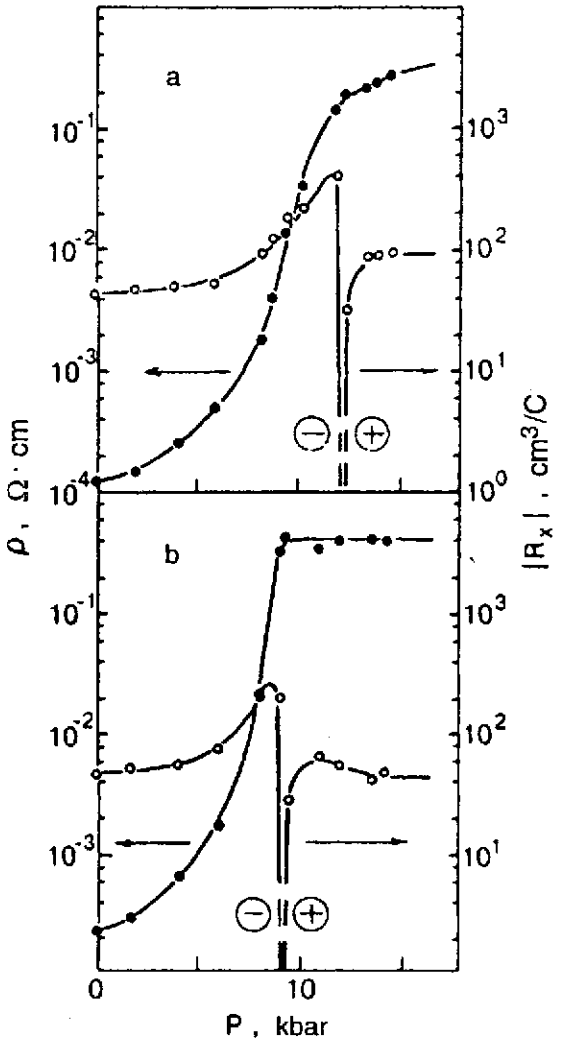

FIG. 5. Pressure dependence of resistivity and Hall constant at $T=4.2$ K for the electron–irradiated sample W-2 (see Table I) for $\Phi\cdot 10^{-17}$, cm^{-2}: 1.6(a);4.0(b).

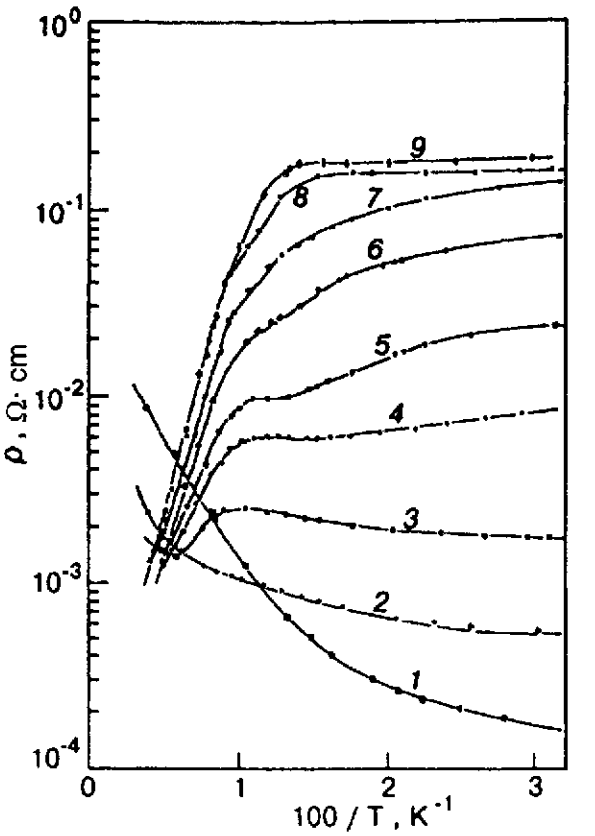

FIG. 6. Temperature dependence of resistivity of the sample W-2 ($\Phi=1.6\cdot 10^{17}$ cm^{-2} during metal–insulator transition under pressure P (kbar): 0 (curve *1*), 5.9 (curve *2*), 8.2 (curve *3*), 9.4 (curve *4*), 10.2 (curve *5*), 11.9 (curve *6*), 12.3 (curve *7*), 13.4 (curve *8*), and 13.9 (curve *9*).

at low temperatures is conduction in the localized states band or surface conduction, both of which are of hole type. Since the electrical and physical parameters of the samples in the insulating state tend to their limiting values, it becomes possible to estimate the Hall mobility of charge carriers in the insulating phase: $\mu_H=100-300$ $cm^2/(V\cdot s)$ at $T=4.2$ K.

The nature of temperatures dependence of the resistivity of irradiated samples changes drastically in the vicinity of the metal–insulator transition (Fig. 6). At low pressures, the $\rho(1/T)$ dependence in all samples is of "metallic" type as in undoped $Pb_{1-x}Sn_xSe$ alloys. With increasing pressure, the $\rho(1/T)$ dependence becomes semiconductor type, and acquires two activation regions whose slopes increase monotonically with pressure. The high-temperature activation region is associated with the intrinsic generation of charge carriers emerging upon a decrease in the free electron concentration under pressure, and the elevation of its slope corresponds to an increase in the band gap of the alloy after band inversion at the point L under pressure.

The emergence of a low-temperature activation region on the $\rho(1/T)$ dependence is due to the fact that the middle of the E_t band intersects the conduction band under pressure and falls in the forbidden gap. Hence an increase in temperature leads to a thermal activation of electrons from the localized states band to the conduction band. The activation energy $\Delta E_t=E_c-E_t$, determined from the slope of the $\rho(1/T)$ dependence, increases monotonically under pressure at a rate close to the rate of variation of the band gap width of the alloy with pressure (Fig. 7). This circumstance points towards the constant position of the local band relative to top of the valence band L_6^- and is a direct confirmation of the above assumption.

4.2. Structure of the radiation defect band

An analysis of the available experimental results points towards a significant blurring of the radiation defect band induced by electron irradiation, the blurring being of the same order as in the band gap in the investigated $Pb_{1-x}Sn_xSe$ alloys. Among other things, the pressure corresponding to the metal–insulator transition in electron-irradiated samples varies over a considerable range ($P^*=9-16$ kbar) and depends on the relation between the initial concentration of electrons and the total capacity of the E_t band, i.e., on the magnitude of the radiation flux.

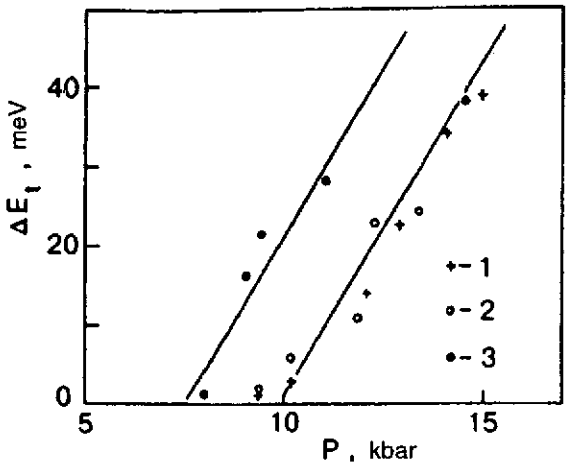

FIG. 7. Pressure dependence of the local band activation energy in electron-irradiated alloys $Pb_{1-x}Sn_xSe$ ($x=0.125$) (solid curves were calculated under the assumption $d\Delta E_t/dP=dE_g/dP=8.5$ meV/kbar): W-0 ($\Phi=4.1\cdot10^{17}$ cm^{-2} (curve *1*), W-2 ($\Phi=1.6\cdot10^{17}$ cm^{-2} (curve *2*), W-2 ($\Phi=4.0\cdot10^{17}$ cm^{-2} (curve *3*).

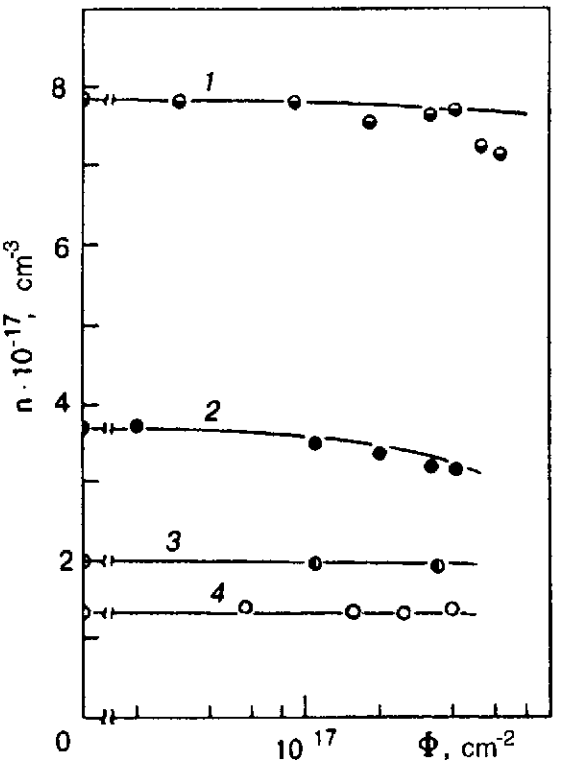

FIG. 8. Dependence of electron concentration in $Pb_{1-x}Sn_xSe$ alloys at $T=4.2$ K on the radiation flux ($x=0.07$ (curve *1*, sample K-12); $x=0.125$ (curve *2*, sample W-0, curve *3*, sample W-11, curve *4*, sample W-2).

Under these conditions, the width of the resonant band emerging as a result of electron irradiation of alloys, as well as its position on the energy scale, can be determined by studying the dependence of the electron concentration in the irradiated alloys on the radiation flux and pressure. Moreover, the well-known energy–momentum relation in the $Pb_{1-x}Sn_xSe$ alloys offers a unique possibility of studying the resonant band structure and reconstructing the density of states in it.[4,43] Finally, a comparison of the pressure dependence of the electron concentration obtained by studying the same sample irradiated by various electron fluxes provides information about the rate of generation of defects due to irradiation.

Figures 8, 9, and 10 show the dependence of the electron concentration in n-$Pb_{1-x}Sn_xSe$ samples ($x=0.07,0.125$) on the radiation flux and pressure, calculated from the experimental values of the Hall constant at $T=4.2$ K. A slow decrease in the concentration of electrons as a result of irradiation indicates that the middle of the local band E_t is much higher than the Fermi level in the investigated samples and has a considerable width ($\simeq 10$ meV) (Figs. 3 and 4). An increase in the radiation flux leads to an increase in the density of localized states and trapping of free electrons by the free states at the tail of the density of states resonance band. The free electron concentration decreases slowly with increasing radiation flux, the maximum variation in the electron concentration occurring in crystals with the highest initial charge concentration.

The experimental pressure dependence of the electron concentration in irradiated samples was constructed by considering the fact that a decrease in the electron concentration in the conduction band leads to a relative increase in the contribution of hole conductivity (conductivity in the radiation defect band or surface conductivity) to the quantities ρ and R_X being measured in a weak magnetic field at $T=4.2$ K. Hence the electron concentration $n(P)$ was calculated by using the two-band model

$$R_X=\frac{\sigma_p\mu_p-\sigma_n\mu_n}{(\sigma_p+\sigma_n)^2}, \tag{3}$$

$$1/\rho=\sigma_p+\sigma_n, \quad n=\sigma_n/e\mu_n. \tag{4}$$

The limiting values of the Hall mobility and conductivity in each sample in the insulating phase ($P>P^*$) were taken for the mobility μ_p in the case of local band conductivity and for hole conductivity σ_p. The mean values of these parameters were used for samples with $N_t<n_0$, in which the metal–insulator transition is not realized under pressure.

The theoretical dependences (solid curves in Figs. 8, 9, and 10) were obtained under the assumption that the defect generation rate $dN_t/d\Phi$ is independent of the radiation flux, the middle of the resonance band E_t remains fixed relative to the energy level L_6^- under pressure, and the density of states function $g_t(E)$ in the resonance band is described by a Gaussian-type curve:

$$g_t(E)=\frac{1}{\sigma\sqrt{2\pi}}\frac{dN_t}{d\Phi}\,\Phi\,\exp\left[-\frac{(E-E_t)^2}{2\sigma^2}\right], \tag{5}$$

where σ is the resonant band width.

Since the experiments indicate a flow of electrons from the conduction band to the resonant band of irradiated alloys both upon an increase in the radiation flux and under hydrostatic pressure, it was also assumed that for all values of Φ and P, the sum of electron concentrations n and n_t in the conduction band and resonant band is equal to the initial electron concentration n_0 in the sample:

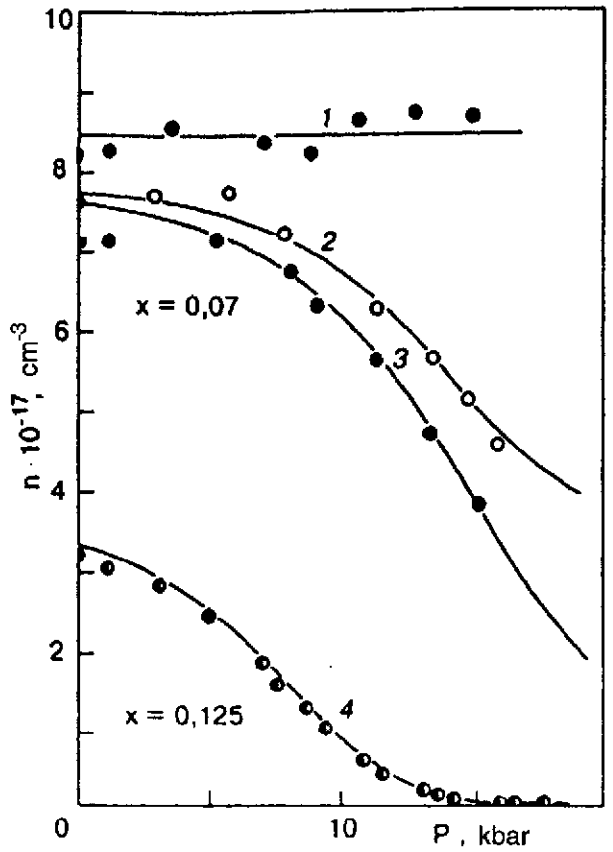

FIG. 9. Pressure dependence of electron concentration in electron-irradiated $Pb_{1-x}Sn_xSe$ samples at $T=4.2$ K($N_t<n_0$) ($x=0.07$: curve *1*, sample K-11 ($\Phi=0$), curve *2*, sample K-12 ($\Phi=3.3\cdot10^{17}$ cm^{-2}), curve *3*, sample K-12 ($\Phi=6.2\cdot10^{17}$ cm^{-2}); $x=0.125$: curve *4*, sample W-0 ($\Phi=3.3\times10^{17}$cm^{-2}).

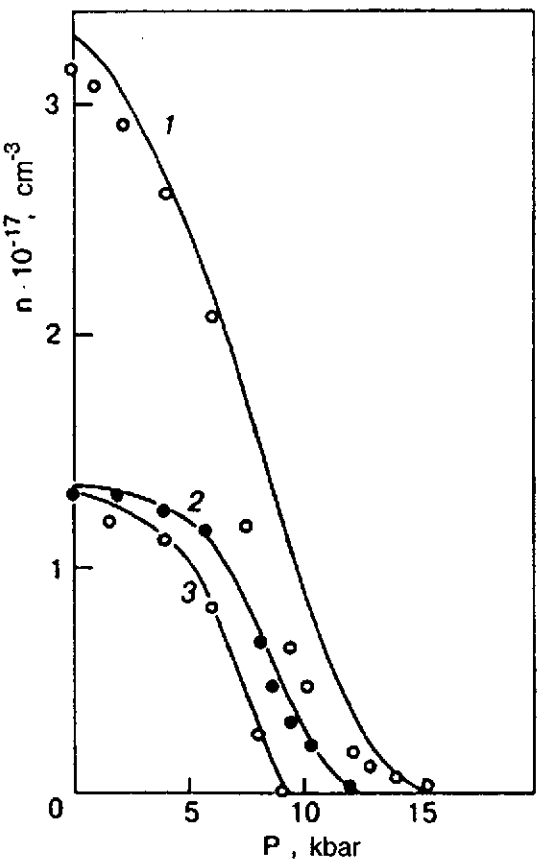

FIG. 10. Pressure dependence of electron concentration in electron-irradiated $Pb_{1-x}Sn_xSe$ ($x=0.125$) samples at $T=4.2$ K($N_t>n_0$) curve *1* sample W-0 ($\Phi=4.1\cdot10^{17}$ cm^{-2}), curve *2*, sample W-2 ($\Phi=1.6\cdot10^{17}$ cm^{-2}), curve *3*, sample W-2 ($\Phi=4.0\cdot10^{17}$ cm^{-2}).

$$n_0=n(P)+n_t(P), \quad n_t(P)=\int_{-\infty}^{E_F} g_t(E)dE, \tag{6}$$

where E_F, the Fermi energy in the irradiated samples, is a function of the radiation flux and pressure.

The position of the Fermi level in irradiated samples was calculated by using Dimmock's energy–momentum relation taking into account the dependence of the parameters $E_\perp$ and $E_\parallel$ on the alloy composition.[4,43] It must be noted that the possibility of using the well-known energy–momentum relation for charge carriers at the point L is of fundamental importance, since it allows us to calculate the theoretical dependences $n(\Phi)$ and $n(P)$ in irradiated samples with the required accuracy and to determine the resonant band parameters in $Pb_{1-x}Sn_xSe$ alloys ($x=0.07,0.125$).

The best agreement between the theory (solid curves in Figs. 8, 9, and 10) and the experiment was obtained for model parameters presented in Table I under the assumption that under atmospheric pressure, the middle of the resonant band lies in the conduction band: $E_t\equiv E_c+70$ meV for $Pb_{1-x}Sn_xSe$ alloys ($x=0.07$) and $E_t\equiv E_c+56$ meV for $Pb_{1-x}Sn_xSe$ alloys ($x=0.125$). The theoretical dependences constructed by using this model are in good agreement with the experimental data.

An analysis of resonant band parameters (Table I) shows that the rate of defect generation as a result of irradiation is $dN_t/d\Phi\simeq1$ cm^{-1} for all investigated samples. This means that in order to attain density of resonant states comparable with those typical of $Pb_{1-x}Sn_xSe$ alloys ($n,p\equiv10^{17}$–10^{18} cm^{-3}), the samples must be exposed to an electron flux $\Phi\equiv10^{17}$–10^{18} cm^{-2}. An increase in the radiation flux apparently points towards a slow decrease in the resonant states generation rate and an insignificant increase in the resonant band width without any change in the form of the function of density of states in it. Hence the assumption concerning a constant generation rate for resonant states and an unchanged form of the density of states function in the resonant band used in calculations do not contradict the available data and must not exert a considerable effect on the results of calculations.

5. RADIATION DEFECT BAND IN ELECTRON-IRRADIATED ALLOYS $Pb_{1-x}Sn_xSe$ WITH AN INVERSE SPECTRUM

According to the energy spectrum model of electron-irradiated alloys $Pb_{1-x}Sn_xSe$, the position of the radiation defect band E_t changes relative to the energy level L_6^- upon an increase in tin concentration (Fig. 1). In a certain range of compositions, the middle of the E_t band in alloys with an inverse spectrum ($E_g<0$) must lie in the forbidden band. In this case, it is possible to observe a pressure-induced metal–insulator transition caused by a flow of electrons from the

TABLE I. Resonance band parameters of electron-irradiated alloys n-$Pb_{1-x}Sn_xSe$.

Sample	x	$n_0 \cdot 10^{-17}$, cm^{-3}	$\Phi \cdot 10^{-17}$, cm^{-2}	$dN_t/d\Phi$, cm^{-1}	σ, meV
K-12	0.07	7.80	3.3	1.20	18
			6.2	1.05	20
W-0	0.125	3.70	3.3	1.10	20
			4.1	0.90	20
W-11	0.125	2.00	3.5	0.57	13
W-2	0.125	1.35	1.6	0.90	13
			4.0	0.75	15

conduction band to the radiation defect band, as well as a redistribution of electrons between the radiation defect band and one of the allowed bands during reconstruction of the energy spectrum of electron-irradiated alloys under pressure.

To observe these effects experimentally and to construct the energy level diagram of irradiated alloys right up to the boundary of existence of the cubic phase, the effect of electron irradiation of alloys with tin concentration $0.2 \leqslant x \leqslant 0.34$ followed by hydrostatic compression was studied in Refs. 42, 44–51.

5.1. Metal-insulator transition induced by electron-irradiation of alloys n-$Pb_{1-x}Sn_xSe$ ($x=0.2,0.25$)

It is found that electron irradiation of alloys leads to the emergence in the band gap of a radiation defect band E_t which is not filled by electrons (Fig. 11). The generation of defects due to irradiation leads to an increase in the density of localized states, flow of electrons from the conduction band to the band E_t, and a decrease in the concentration of free electrons in the investigated samples. In alloys with $x=0.25$ and for radiation flux $\Phi=\Phi^*$, the electron concentration becomes equal to zero and a metal–insulator transition takes place (Fig. 12). In the insulating phase ($\Phi>\Phi^*$), the Fermi level is stabilized in the E_t band while the electrical and physical parameters of the alloys attain limiting values that are practically independent of the radiation flux.

At the same time, the radiation defect band in alloys with $x=0.2$ lies in the forbidden gap near the bottom of the conduction band L_6^+ and strongly overlaps with the conduction band, forming a single band of allowed states. This circumstance, as well as high initial concentration of electrons in the samples makes it extremely difficult to observe the transition to the insulating state and to determine exactly the position of the E_t band in these alloys on the energy scale.

The nature of the dependence of electrical and physical parameters of investigated samples on radiation flux changes in the vicinity of the metal–insulator transition (Fig. 13): the resistivity tends to saturation, the Hall constant decreases in magnitude and suffers inversion, while the Hall mobility of charge carriers, which remained practically unchanged in the radiation flux region $\Phi<\Phi^*$, decreases by more than an order of magnitude. Subsequent exposure to an electron flux about twice the value of Φ^* practically does not change the

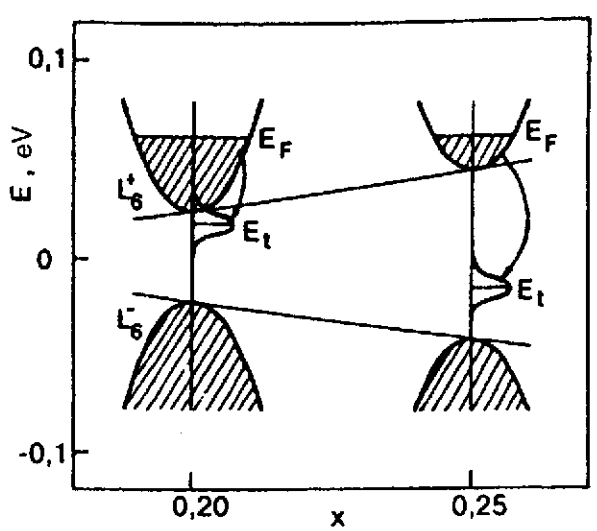

FIG. 11. Model of energy spectrum of electron-irradiated alloys n-$Pb_{1-x}Sn_xSe$ ($x=0.2,0.25$).

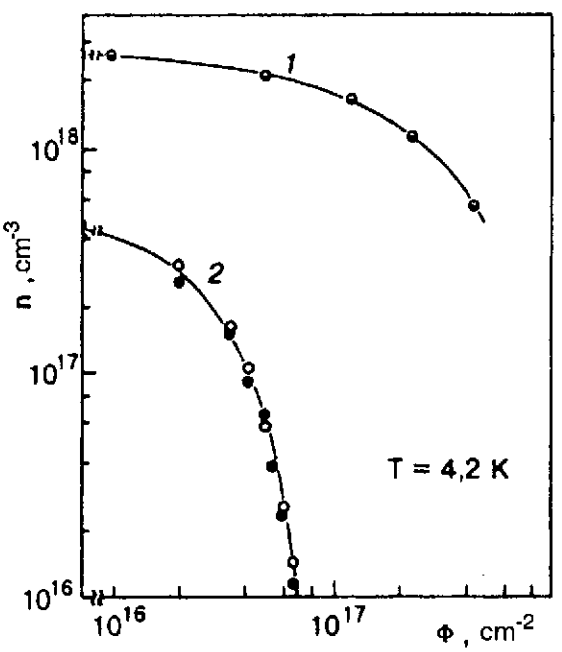

FIG. 12. Dependence of electron concentration in n-$Pb_{1-x}Sn_xSe$ samples with inverse spectrum at $T=4.2$ K on the radiation flux: $x=0.2$ (curve 1), $x=0.25$ (curve 2).

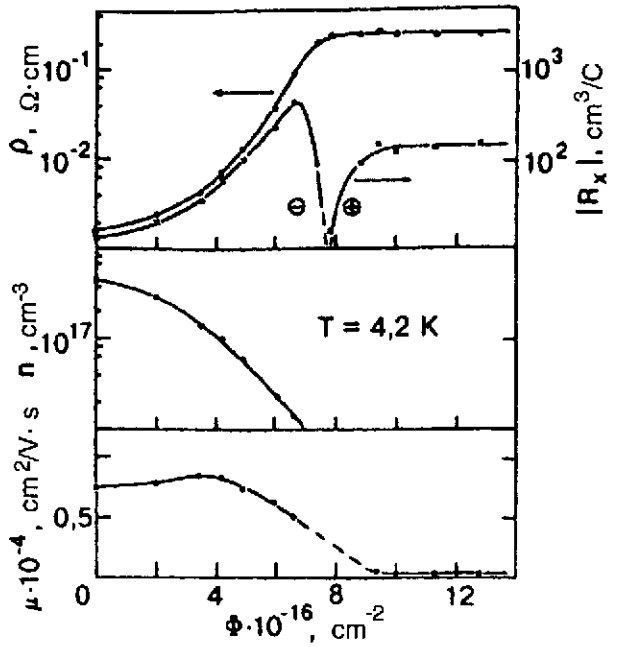

FIG. 13. Dependence of electrical and physical parameters of n-$Pb_{1-x}Sn_xSe$ ($x=0.25$) samples on radiation flux at $T=4.2$ K.

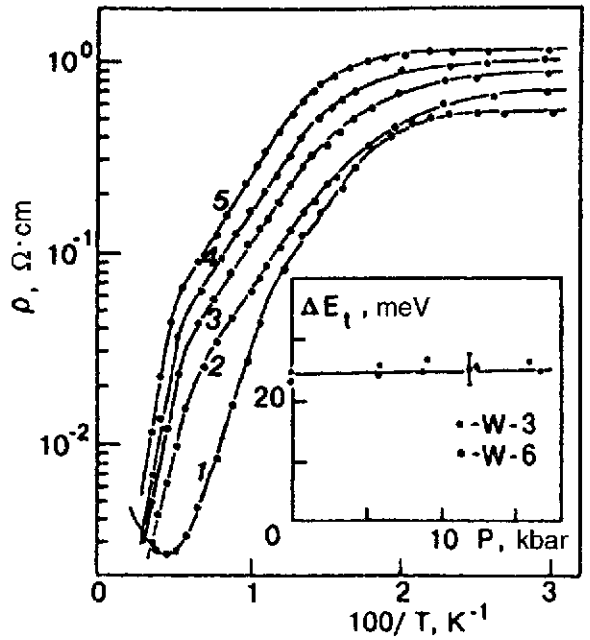

FIG. 14. Temperature dependence of resistivity of the sample W-6 ($x=0.25$, $\Phi=2\cdot10^{17}$ cm^{-2}) under pressure P (kbar): 0 (curve *1*), 5.8 (curve *2*), 8.8 (curve *3*), 12.1 (curve *4*), 16.2 (curve *5*). The inset shows the pressure dependence of the activation energy of the local level in electron-irradiated samples of n-$Pb_{1-x}Sn_xSe$ ($x=0.25$).

electrical and physical parameters of crystals, which points towards a certain limiting state and stabilization of the Fermi level.

At helium temperatures, the Hall constant is positive in the insulating phase, thus pointing towards a hole-type conductivity. However, the Hall mobility in the insulating phase ($\mu_H=10^2-10^3$ $cm^2/V\cdot s$ at $T=4.2$ K) is more than an order of magnitude lower than the free hole mobility at L. Hence it can be assumed that in the insulating phase, the main conductivity mechanism at low temperatures is the conductivity over the localized states band, which is of hole type. Alternatively, the positive sign of the Hall constant in the insulating phase is explained by the assumption about the formation of an inversion layer with p-type conductivity on the sample surface. In principle, such a surface layer can be formed in the samples as a result of chemical treatment of the surface or by exposure to fast electrons (surface oxidation, surface defects).

The application of hydrostatic pressure[49] provides additional information on the behavior of electrical and physical parameters of electron-irradiated alloys in the insulating phase, as well as by the position of the radiation defect band relative to the allowed band edge at L on the energy scale in electron-irradiated samples $Pb_{1-x}Sn_xSe$ ($x=0.25$).

Among other things, it is found that the temperature dependence of resistivity in the insulating phase is characterized by the emergence of two characteristic activation regions whose slopes differ by a factor of two (Fig. 14). The slope of the high-temperature region increases monotonically with pressure, while that of the low-temperature region remains practically unchanged upon the application of pressure. The activation energy and the rate of its variation with pressure determined from the slope of the high-temperature activation region lead to the assumption that this segment corresponds to intrinsic ionization of charge carriers, while an increase in its slope is associated with an increase in the band gap of the alloy under pressure (under atmospheric pressure, the band gap in the investigated alloys is $E_g\simeq85$ meV at $T=4.2$ K). The slope of the low-temperature activation segment on the dependence $\rho(1/T)$ is determined by the separation between the middle of the E_t band and the top of the valence band E_v. The activation energy, calculated from the slope of the dependence $\rho(1/T)$ in investigated samples is $\Delta E_t=E_t-E_v=(24\pm3)$ meV and is practically independent of pressure.

The constancy of the activation energy ΔE_t in the investigated pressure range suggests that the position of the localized states band relative to the energy level L_6^- (top of the valence band) practically does not change with pressure. An identical behavior was observed under pressure in the band of radiation defects induced by electron irradiation in the energy spectrum of the alloys $Pb_{1-x}Sn_xSe$ ($x=0.125$). This circumstance is yet another confirmation of the fact that the radiation defect bands observed in electron-irradiated alloys $Pb_{1-x}Sn_xSe$ with direct and inverse spectra are of the same origin. The position of this band relative to the energy level L_6^- depends almost linearly on the alloy composition [$E_t\simeq L_6^-+(87-250x)$ meV] and does not change as a result of compression.

5.2. Parameters of radiation effect bands in electron-irradiated alloys p-$Pb_{1-x}Sn_xSe$ ($x=0.34$)

According to the energy-level diagram presented in Fig. 1, it can be expected that the radiation defect band in alloys $Pb_{1-x}Sn_xSe$ ($x=0.34$) lies near the top of the valence band against the background of allowed states of the valence band (Fig. 15).

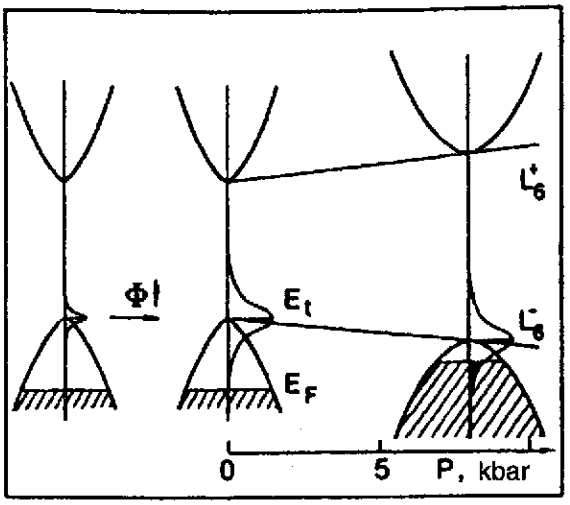

FIG. 15. Reconstruction of energy spectrum of the electron-irradiated alloy p-$Pb_{1-x}Sn_xSe$ ($x=0.34$) under uniform compression.

An increase in the radiation flux leads to an increase in the capacity of the band E_t and trapping of electrons from the valence band at unfilled states in the tail of the density of states in the radiation defect band. For a high hole concentration in the samples, however, irradiation does not cause a significant change in the hole concentration (Fig. 16) which is determined by the overlapping of the tail of the density of states function for the radiation defect band with filled states in the valence band. Under pressure, the band E_t moves parallel to the top of the valence band. Hence an increase in hole concentration (Fig. 16) occurs only due to an increase in the density of states in the valence band, as a result of which the Fermi level approaches the top of the valence band, the overlapping of the radiation defect band with filled states in the valence band increases, and a part of electrons flows from the valence band to the radiation defect band.

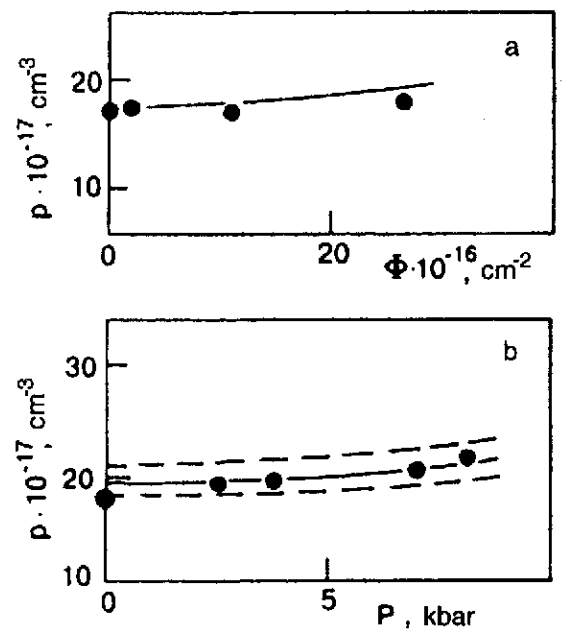

FIG. 16. Dependence of hole concentration and of p-$Pb_{1-x}Sn_xSe$ ($x=0.34$) samples on radiation flux (a) and pressure (b) ($\Phi=2.7\cdot10^{17}$ cm^{-2}) at $T=4.2$ K. The solid curves were calculated for $E_t-E_v=0$, $\sigma=13$ meV, $dN_t/d\Phi=6$ cm^{-2}, while the dashed curves correspond to $E_tE_v=\pm5$ meV, $\sigma=13$ meV, $dN_t/d\Phi=6$ cm^{-2}.

The dependence of the hole concentration on radiation flux and pressure was used for determining the parameters of the energy spectrum model for irradiated alloys.[50,51] However, it is hard to determine independently the numerical values of all parameters in the radiation defect band for the alloy $Pb_{1-x}Sn_xSe$ ($x=0.34$) due to a weak sensitivity of the hole concentration dependence on radiation flux and pressure to the E_t band parameters. As a matter of fact, the maximum increase in the hole concentration under pressure does not exceed 30% since a pressure $P\simeq8$ kbar leads to an abrupt change in the electrical and physical parameters due to a structural phase transition to an SnSe type lattice.[52,53] Hence a comparison of theoretical results (solid curves in Fig. 16) with the experimental data is made under the assumption that the position of the middle of the E_t band coincides with the top of the valence band and by using the values of radiation defect band parameters (resonance band width σ and the generation rate $dN_t/d\Phi$ of the states as a result of irradiation) characteristic of thoroughly investigated alloys $Pb_{1-x}Sn_xSe$ ($0.07\leqslant x\leqslant0.25$): $\sigma\simeq13$ meV and $dN_t/d\Phi\simeq6$ cm^{-1}. Calculations were made by using the condition of electrical neutrality:

$$p(\Phi,P)=p_0+N_t(\Phi)-p_t(\Phi,P),$$

$$p_t(\Phi,P)=\int_{E_F}^{\infty}g_t(E)dE, \qquad (7)$$

where p_0 is the initial hole concentration in the sample, $p_t(\Phi,P)$ the hole concentration in the radiation defect band, $g_t(E)$ the density of states function in the radiation defects band, and E_F the Fermi energy calculated according to Dimmock's energy–momentum relation with the values of parameters presented in Ref. 4.

It is also assumed that the total capacity of the radiation defects band depends linearly on the radiation flux $[N_t=\Phi(dN_t/d\Phi)]$, while the density of states function $g_t(E)$ in the resonance band can be approximated by the Gaussian-type curve (5).

In order to estimate the reliability of the obtained results, similar calculations were also made by varying the position of the middle of the E_t band relative to the top of the valence band (dashed curve in Fig. 16). These calculations showed that the middle of the E_t band in the investigated alloy practically coincides with the top of the valence band at the point $L(E_t\simeq L_6^-\pm5$ meV), thus permitting the use of the above diagram of movement of the radiation defects band relative to the edges of the allowed bands at L almost right up to the boundary of the range of the cubic phase ($x<0.41$).

6. INSULATOR–METAL TRANSITION IN ELECTRON-IRRADIATED ALLOYS $Pb_{1-x}Sn_xSe$ ($x\leqslant0.03$)

The experimental data on the structure of the radiation defect band E_{t1} and its position on the energy scale in electron-irradiated alloys $Pb_{1-x}Sn_xSe$ ($x=0;0.03$) were obtained in Refs. 30, 54 and 55.

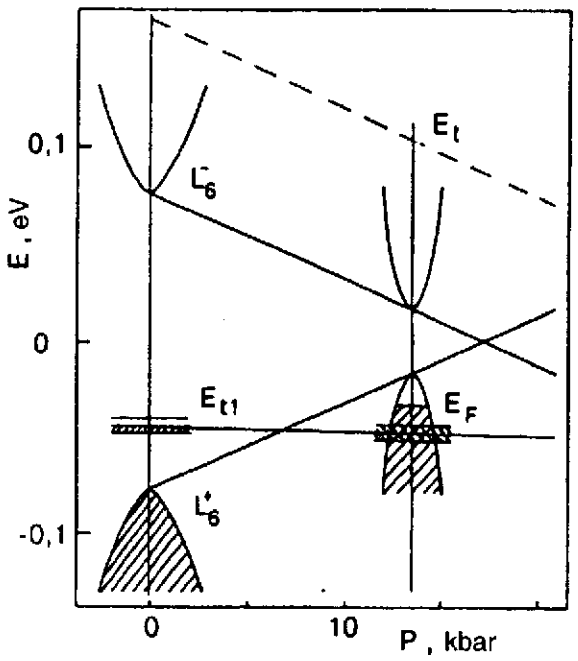

FIG. 17. Reconstruction of energy spectrum of electron-irradiated alloys $Pb_{1-x}Sn_xSe$ under pressure.

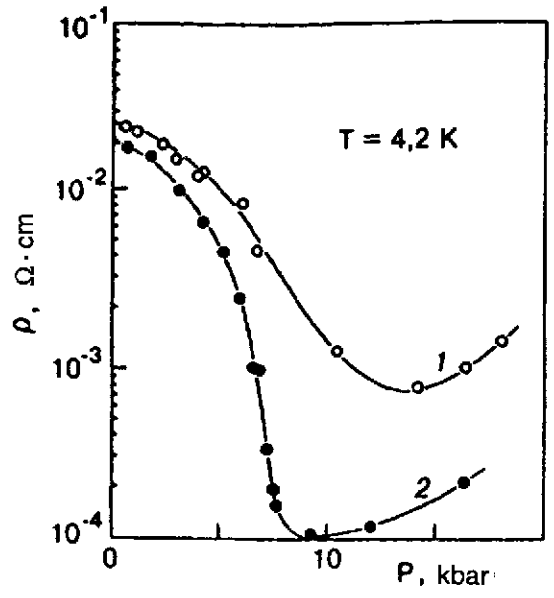

FIG. 18. Pressure dependence of resistivity of electron-irradiated $Pb_{1-x}Sn_xSe$ samples at $T=4.2$ K: sample K-22 ($x=0.03$, $\Phi=2.8\cdot10^{17}$ cm^{-2} (curve *1*)), sample N8 [$x=0$, $\Phi=5.7\cdot10^{17}$ cm^{-2} (curve *2*)].

It was found that, irrespective of the type of conductivity of the initial crystals, the electron-irradiated alloys under atmospheric pressure are in the insulating state in which the valence band is completely filled with electrons at low temperatures, the conduction band is free of electrons, and the E_{t1}-band is partially filled with electrons (Fig. 17). Under uniform compression, the middle of the local band E_{t1} in the irradiated alloys approaches the valence band and intersects the top of the valence band L_6^+, inducing an increase in the free hole concentration as a result of redistribution of charge carriers between the valence band and the bands of charged states, and the insulator–metal transition under pressure. In the region of maximum compression, the local band is found to be filled by electrons completely and lies in the valence band below the Fermi level, while the concentration of free holes attains saturation and is practically independent of pressure.

The insulator–metal transition is accompanied by significant variations of the electrical and physical parameters of the irradiated samples (Figs. 18 and 19). Under hydrostatic pressure, the resistivity of irradiated samples decreases at $T=4.2$ K by about two orders of magnitude and passes through a minimum in the pressure interval $P=9$–14 kbar. The magnitude of the Hall constant R_X decreases sharply and undergoes inversion at a certain value $P=P_k$. In the region of maximum compression, the Hall constant attains saturation and is positive.

It must be remarked that the mobility of charge carriers in the electron–irradiated samples in the insulating phase have very low values (10^3–10^4 cm^2/(V·s) for the $Pb_{1-x}Sn_xSe$ alloys. These values of the electron mobility are preserved under low pressures ($P<P_k$). Immediately after the n–p conversion (in the metallic phase), however, the mobility of charge carriers increases sharply by more than an order of magnitude and attains values typical of undoped $Pb_{1-x}Sn_xSe$ alloys. All the investigated samples acquire clear transverse magnetoresistance oscillations in quantizing magnetic fields (Fig. 20). In a narrow pressure interval, the amplitude and frequency of Shubnikov oscillations increase sharply, while the free hole concentration calculated from the oscillation periods $\Delta_{100}(1/B)$ coincide to within 10% with the values calculated from the Hall constant R_X and attains saturation upon an increase in pressure.

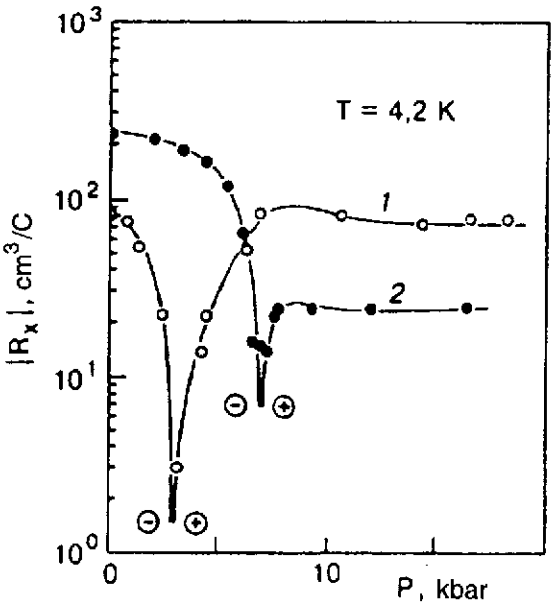

FIG. 19. Pressure dependence of the Hall constant of electron-irradiated $Pb_{1-x}Sn_xSe$ samples at $T=4.2$ K: sample K-22 ($x=0.03$, $\Phi=2.8\cdot10^{17}$ cm^{-2} (curve *1*)), sample N8 ($x=0$, $\Phi=5.7\cdot10^{17}$ cm^{-2} [curve *2*)].

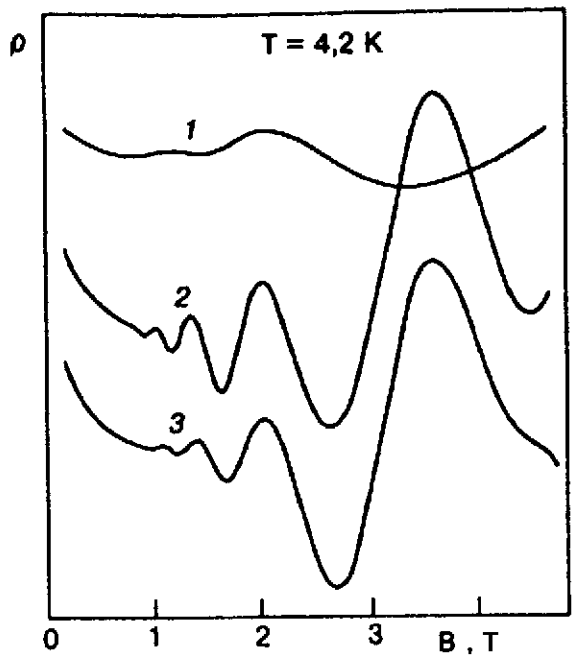

FIG. 20. Transverse magnetoresistance oscillations of the electron-irradiated sample N8 at $T=4.2$ K ($x=0$, $\Phi=5.7\cdot10^{17}$ cm^{-2}) under pressure P (kbar): 6.9 (curve *1*), 7.7 (curve *2*), 16.4 (curve *3*).

The obtained results indicate that the negative sign of R_X in the insulating phase at low temperatures cannot be due to the existence of free electrons since the mobility of charge carriers in irradiated samples was found to be much lower than in unirradiated samples, and also lower than in irradiated samples under compression. Apparently, the main conductivity mechanism in the insulating phase at low temperatures is the surface conductivity or conductivity in the localized states band located in the band gap of the alloys.

A comparison of the experimental data obtained for alloys with $x=0$ and $x=0.03$ shows that the activation energy of the E_{t1} level depends on the alloy composition and pressure (Fig. 21), while the inversion of the sign of the Hall

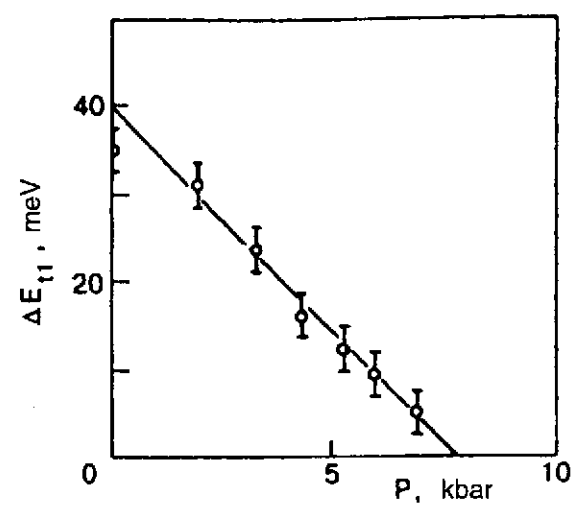

FIG. 21. Pressure dependence of the activation energy of the deep level E_{t1} in electron-irradiated sample N8 ($x=0$, $\Phi=5.7\cdot10^{17}$ cm^{-2}).

constant corresponding to the point of intersection of the E_{t1} level with the top of the L_6^+ band takes place in both alloys for the same band gap E_g ($P_k\simeq7$ kbar for PbSe and $P_k\simeq3$ kbar for the alloys $Pb_{1-x}Sn_xSe$ ($x=0.03$)). These results were used to estimate the rate of displacement of the middle of the E_{t1} band relative to the top of the valence band L_6^+ upon a change in the tin concentration and pressure. It was found that under hydrostatic compression, $d(\Delta E_{t1})/dP\simeq-5$ meV/kbar, and the E_{t1} band slowly moves downwards relative to the middle of the band gap. Upon an increase in the tin concentration in the alloy, the middle of the E_{t1} band also moves downwards slowly relative to the middle of the band gap and its position relative to the energy level L_6^+ varies almost linearly: $E_{t1}\simeq L_6^+ + (40-700x)$ meV, and falls in the valence band for $x>0.06$.

It should also be observed that in the vicinity of the insulator–metal transition, significant variation of the charge carrier parameters occurs in a wide pressure range $\Delta P=3-4$ kbar (Figs. 18 and 19). This circumstance points towards a finite width of the E_{t1} band and permits the use of the pressure dependence of hole concentration in irradiated alloys for reconstructing the density of states function in the E_{t1} band. However, calculation of the $p(P)$ dependences from the experimental dependences $\rho(P)$ and $R_X(P)$ is considerably hampered by the additional electron-type conductivity mechanism in the insulating phase, which is probably associated with the surface conductivity. Estimates show that under the assumption of the Gaussian form of the density of states function in the radiation defects band, the E_{t1} band is several times narrower than the E_t band and its width amounts to $\sigma=3-7$ meV.

7. RESONANCE BAND OF RADIATION DEFECTS IN ELECTRON-IRRADIATED $Pb_{1-x}Sn_xTe$ ($x\simeq0.2$) ALLOYS

It is well known that hydrostatic compression of $Pb_{1-x}Sn_xTe$ ($x<0.35$) alloys reduces the band gap and leads to the inversion of energy levels at the point L. The concentration of charge carriers remains unchanged in undoped and nonirradiated crystals,[11,56] but the compression of electron-irradiated $Pb_{1-x}Sn_xTe$ ($x\simeq0.2$) alloys, whose energy spectrum contains a wide resonant band of radiation defects, must lead to a change in the mutual arrangement of allowed bands at L and the resonant band, thus inducing a rearrangement of electrons between them and a change in the free charge carrier concentration.

The most comprehensive information about the radiation defect band in $Pb_{1-x}Sn_xTe$ alloys was obtained by studying the effect of electron irradiation and subsequent uniform compression on the electrical and physical properties of $Pb_{1-x}Sn_xTe$ ($x=0.2,0.22$) alloys of n- and p-type.[31,32,41,57,58]

7.1. Reconstruction of the energy spectrum under pressure

It has been found that when electron-irradiated samples of $Pb_{1-x}Sn_xTe$ ($x=0.2,0.22$) are subjected to hydrostatic compression, the hole concentration increases monotonically in all of them and tends to saturation (Fig. 22). From the

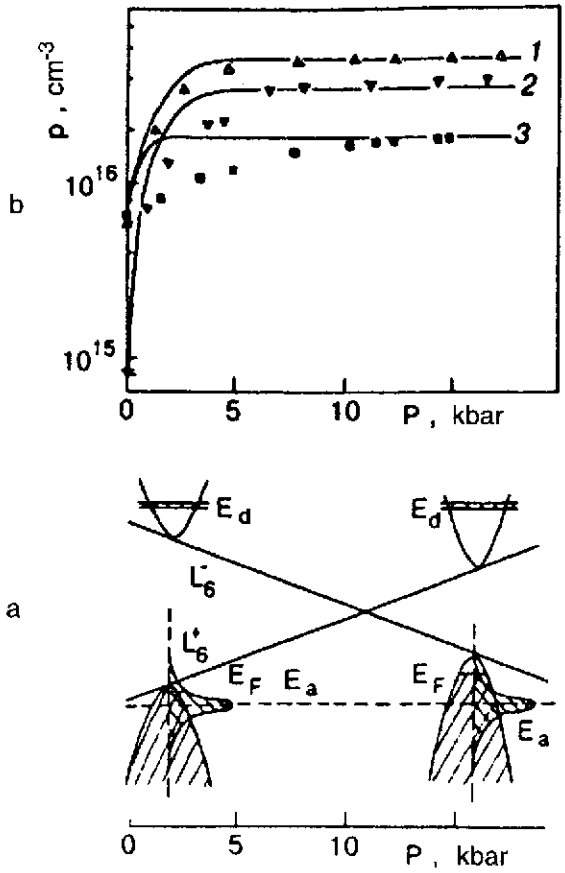

FIG. 22. Pressure dependence of the hole concentration in electron-irradiated p-$Pb_{1-x}Sn_xSe$ samples ($x=0.2$) at $T=4.2$ K (a): sample sp-2 ($\Phi=2.2\cdot10^{17}$ cm^{-2} (curve *1*), sample sp-2 ($\Phi=3.35\cdot10^{17}$ cm^{-2} (curve *2*), and sample p-11 ($\Phi=1.4\cdot10^{17}$ cm^{-2} (curve *3*); diagram showing the reconstruction of the energy spectrum of the alloy under pressure (b).

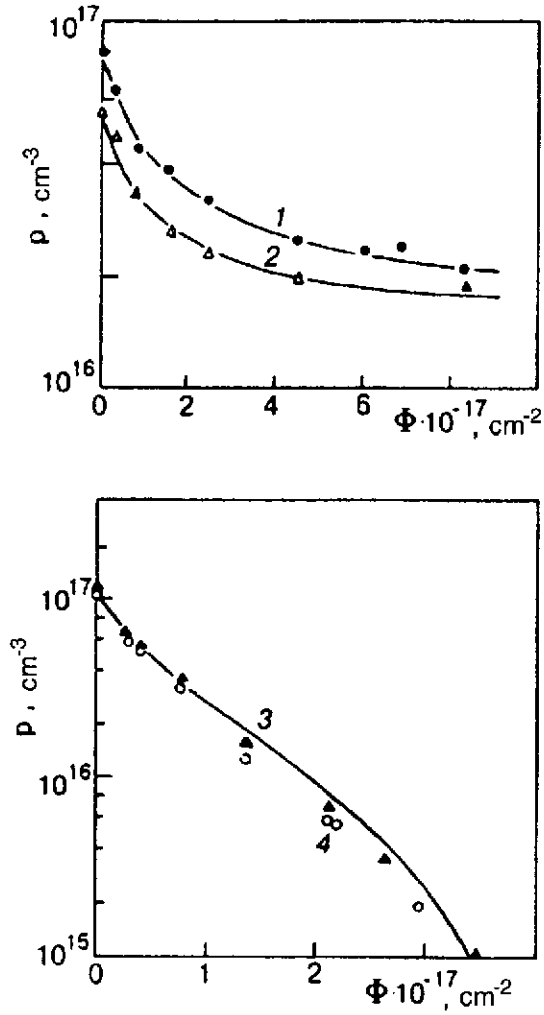

FIG. 23. Dependence of the hole concentration in p-$Pb_{1-x}Sn_xSe$ samples on radiation flux at $T=4.2$ K: sample p-1 (curve *1*), sample p-2 (curve *2*), sample sp-1 (curve *3*), sample sp-2 (curve *4*). The solid curves are the results of calculations based on the model with parameters presented in Table II.

point of view of the energy spectrum model of electron-irradiated $Pb_{1-x}Sn_xTe$ ($x=0.2$) alloys (Fig. 22), an increase in the hole concentration under pressure is possible upon an increase in the separation between the top of the valence band and the middle of the resonant band, say, for an unchanged position of the resonant band relative to the middle of band gap under pressure. In this case, the resonant band is "immersed" into the valence band upon an increase in pressure, collects a part of electrons from the valence band, and increases the free hole concentration in the valence band.

Preliminary calculations show that the form of the $p(P)$ dependence is determined by the concentration of the unfilled states in the resonant band and mutual arrangement of the middle of the resonant band and the Fermi level in irradiated samples under atmospheric pressure, as well as by the form of the density of states function in the resonant band. In particular, the $p(P)$ dependence for a low capacity of the resonant band must have a plateau in the pressure interval in which all vacancies in the resonant band are occupied by electrons, while the passage of the Fermi level through the middle of the resonant band must lead to the emergence of a characteristic inflection on the $p(P)$ curve, whose absence may indicate that under atmospheric pressure, the middle of the resonant band lies below the Fermi level.

7.2. Parameters of the energy spectrum model

In order to determine the parameters of the energy spectrum model of electron-irradiated alloys $Pb_{1-x}Sn_xTe$ ($x\approx0.2$), it is convenient to use the dependence of the hole concentration in the investigated samples on the radiation flux (Fig. 23) and pressure (Fig. 22). While calculating the dependence of the hole concentration on the radiation flux, it was assumed that a decrease in the hole concentration occurs as a result of the flow of electrons from the donor level E_d to the valence band and the acceptor-type resonant band E_a (Fig. 2). Hence the hole concentration must satisfy the equation

$$p(\Phi)=p_0-[N_d-n_a(\Phi)], \quad n_a(\Phi)=\int_{-\infty}^{E_F} g_a(E)dE, \tag{8}$$

$$g_a(E)=\frac{N_a}{\sigma\sqrt{2\pi}}\exp\left[-\frac{(E-E_a)^2}{2\sigma^2}\right], \tag{9}$$

TABLE II. Energy spectrum parameters of electron-irradiated alloys n $Pb_{1-x}Sn_xTe$.

Sample	x	Type of conductivity	$dN_d/d\Phi$, cm^{-1}	$dN_a/d\Phi$, cm^{-1}	E_v-E_a, meV	σ, meV
p-1	0.2	p	0.65	0.7	6.5	2
p-2	0.2	p	0.65	0.7	6.2	2
p-3	0.2	p	0.7	0.75	6.3	1.9
p-4	0.2	p	0.7	0.75	6.5	2
p-11	0.2	p	0.23	0.17	2.5	1.5
p-12	0.2	p	0.25	0.2	1.8	1
sp-1	0.2	p	1.9	1.7	6.5	4
sp-2	0.2	p	1.9	1.7	6.5	4
c-22	0.22	n	1.67	1.7	9.3	4

where $N_d=\Phi dN_d/d\Phi$, $N_a=\Phi dN_a/d\Phi$, $dN_d/d\Phi$ and $dN_a/d\Phi$ being the generation rate of the donor- and acceptor-type defects during irradiation, $g_a(E)$ the density of states in the acceptor-type resonant band in the form of the Gaussian-type curve, E_a and σ are the middle and the width of the resonant band, and E_F the Fermi energy calculated by using the two-band model with parameters of the energy–momentum relation obtained in Ref. 59.

While constructing the theoretical pressure dependence of hole concentration, it was assumed that the total hole concentration p in the valence band and p_a in the resonant band remains constant during reconstruction of the energy spectrum of the irradiated alloy under pressure, while the hole concentration in the valence band is determined from the equation

$$p(P)+p_a(P)=p(0)+p_a(0). \tag{10}$$

Considering that $p_a(P)=N_a-n_a(P)$, and $p_a(0)=N_a-n_a(0)$, we obtain

$$p(P)=p(0)+[n_a(P)-n_a(0)], \tag{11}$$

$$n_a(P)=\int_{-\infty}^{E_F(P)} g_a(E)dE,$$

$$g_a(E)=\frac{N_a}{\sigma\sqrt{2\pi}}\exp\left[-\frac{(E-E_a)^2}{2\sigma^2}\right], \tag{12}$$

The best agreement between the theory and (solid curves in Figs. 22 and 23) experiment was attained by assuming that the position of the resonant band remains unchanged under pressure relative to the middle of the band gap, and by using the model parameters presented in Table II. However, it must be noted that the theoretical curves differ significantly from the experimental points under low pressures. This may be due to the violation of one or several assumptions made during computations based on the proposed model. It is quite possible that the density of states function in the resonant band may differ from the Gaussian form. Moreover, the assumption concerning the fixed position of the resonant band relative to the middle of the band gap is not undisputable, since the obtained experimental data do not allow a precise calculation of the rate of movement of the resonant band relative to the edges of the allowed bands of the alloys under pressure. A reliable evaluation of this parameter requires a considerable enlargement of the pressure range or analogous investigation of $Pb_{1-x}Sn_xTe$ alloys with a higher concentration of tin.

However, the available experimental data allow evaluation of the range of rate of displacement of the resonant band relative to the middle of the band gap. For this purpose, we calculated the pressure dependence of hole concentration in irradiated samples upon a variation of dE_a/dP (Fig. 24). Calculations show that for negative values of dE_a/dP, the disparity between the theoretical dependences $p(P)$ and the experimental data increases under low pressures. For positive values of dE_a/dP, the agreement between theory and ex-

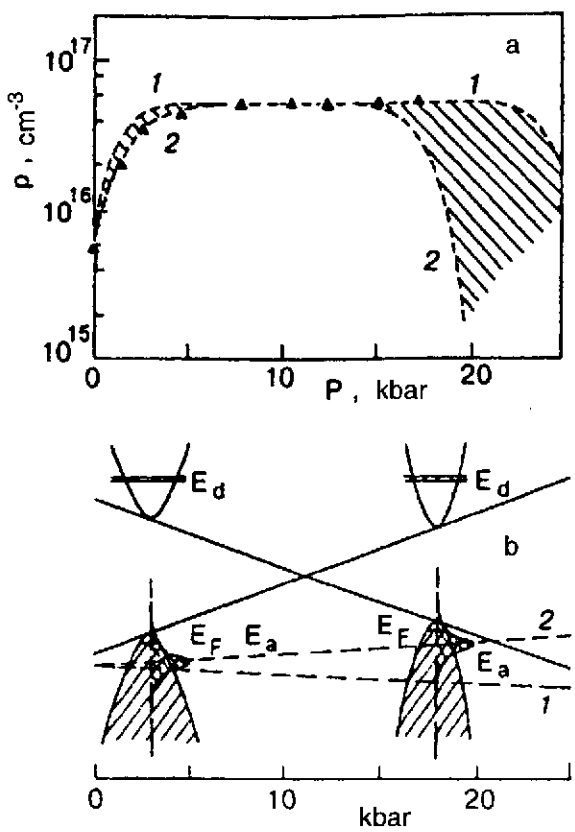

FIG. 24. Dependence of hole concentration at $T=4.2$K in sample sp-2 ($\Phi=2.2\cdot10^{17}$ cm^{-2}) on pressure (a) and upon variation of the rate of displacement of resonance band under pressure (b): $d\Delta E_a/dP$(meV/kbar): −0.5 (curve 1), 0.5 (curve 2).

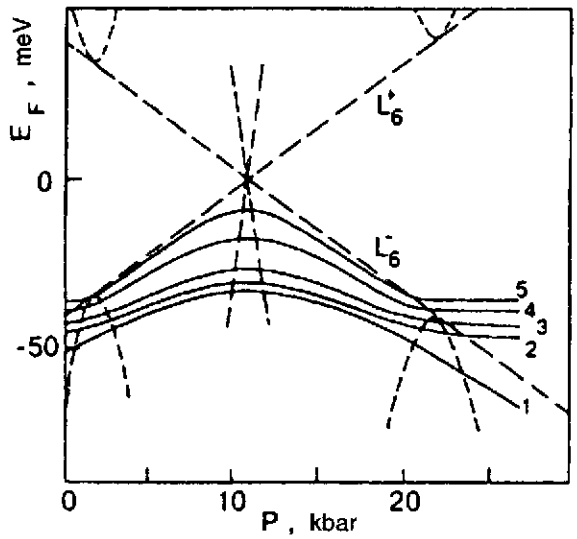

FIG. 25. Pressure dependence of the Fermi level position in $Pb_{1-x}Sn_xTe$ ($x=0.2$)($p_0=1.1\cdot10^{17}$ cm^{-3}) at 4.2 K for different values of radiation flux: $\Phi\cdot10^{-17}$ cm^{-2}: 0 (curve *1*), 1.0 (curve *2*), 2.2 (curve *3*), 4.0 (curve *4*), 4.6 (curve *5*) (calculations made according to the model with parameters characteristic of samples sp-1, 2).

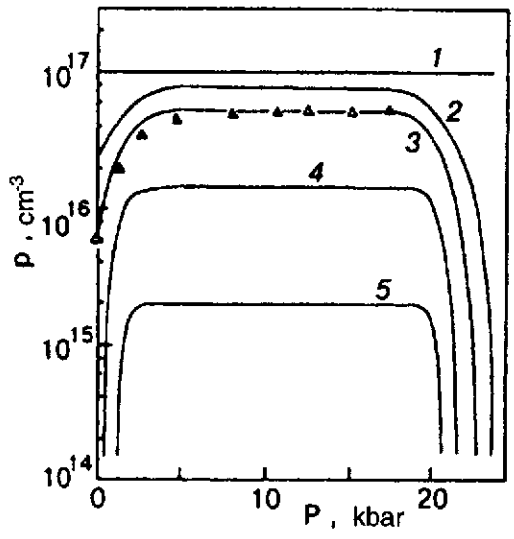

FIG. 26. Pressure dependence of the charge carrier concentration in $Pb_{1-x}Sn_xTe$ ($x=0.2$)($p_0=1.1\cdot10^{17}$ cm^{-3}) at 4.2 K for different values of radiation flux: $\Phi\cdot10^{-17}$ cm^{-2}: 0 (curve *1*), 1.0 (curve *2*), 2.2 (curve *3*), 4.0 (curve *4*), 4.6 (curve *5*) (calculations made according to the model with parameters characteristic of samples sp-1,2).

periment improves under low pressures, but the theoretical dependence deviates sharply from the experimental points in the maximum pressure region. As a matter of fact, the resonant band approaches so close to the top of the valence band L_6^- under pressure for $dE_a/dP>0.5$ meV/kbar that a decrease in the hole concentration and a metal–insulator transition must be observed in the investigated pressure range due to a flow of electrons from the resonant band to the valence band. Hence it can be obviously assumed that the rate of displacement of the resonant band relative to the middle of the band gap is insignificant and does not exceed the value $dE_a/dP=\pm0.5$ meV/kbar.

The above energy spectrum model was used for calculations to predict the behavior of electrical and physical parameters of the alloy under intense irradiation by electrons and subsequent uniform compression. The theoretical pressure dependences of the hole concentration and Fermi level position for electron-irradiated alloy p-$Pb_{1-x}Sn_xTe$ ($x=0.2$) are presented in Figs. 25 and 26. Uniform compression of the irradiated alloys leads to a reconstruction of the energy spectrum of the alloy and a change in the resonant band position relative to the edge of the allowed bands at L (Fig. 25). Before band inversion at the point L, the resonant band moves into the valence band. Hence the hole concentration must increase rapidly due to electron flow from the valence band to the resonant band right until the resonant states are completely filled. After this, the resonant band remains completely filled with electrons over a wide range of pressures about the band inversion point L and does not affect the charge carrier concentration in the alloy. The saturation level and the extent of the hole concentration saturation region are determined by the concentration of the unfilled states in the resonant band under atmospheric pressure and depends on the radiation flux.

After band inversion at the point L, the resonant band approaches the top of the valence band, crosses it and passes into the band gap. In this case, the hole concentration must decrease rapidly due to flow of electrons from the resonant band to the valence band right up to a transition of the samples to the insulating state, and the Fermi level must be stabilized by the resonant band lying in the band gap. The experimental observation of such transitions upon a variation of the radiation flux in the initial samples may provide useful information about the parameters of resonant states induced by electron irradiation in $Pb_{1-x}Sn_xTe$ alloys.

Finally, it must be observed that, for the alloy with $x=0.22$ (the energy is measured from the top of the valence band), the acceptor-type resonance band lies somewhat lower than in the alloy with $x=0.2$ for which the average value of $E_v-E_a\simeq5.3$ meV for the investigated samples. This circumstance leads to the assumption that the position of the resonant band E_a relative to the middle of the band gap in the $Pb_{1-x}Sn_xTe$ alloy is independent of its composition. In this case, the middle of the resonant band intersects the top of the valence band upon a decrease in the tin concentration in the alloy, and falls in the band gap for $x<0.17$. Thus, the electron irradiation of crystals with low tin concentration may lead to stabilization of the Fermi level in the band gap and a transition of the alloys to the insulating state irrespective of the initial type of conductivity.

CONCLUSION

Thus, investigations of electron-irradiated alloys $Pb_{1-x}Sn_xSe$ and $Pb_{1-x}Sn_xTe$ under uniform compression provide detailed information about the energy spectrum of radiation defects in these materials. Among other things, deep and resonant levels of radiation defects have been detected, diagrams of energy spectrum reconstruction have been obtained under pressure and upon variation of the tin concentration in the alloy, as well as the data on the structure

of resonant bands of radiation defects. However, the potentialities of the spectroscopy of localized states under pressure for A^4B^6 semiconductors have not been exploited fully so far.

Investigations over a wide range of tin concentration are needed in order to reconstruct the energy spectrum of electron-irradiated alloys $Pb_{1-x}Sn_xTe$ upon a change in the alloy composition and to observe the above-mentioned metal–insulator type transitions under pressure.

So far, only $Pb_{1-x}Sn_xSe$ and $Pb_{1-x}Sn_xTe$ alloys have been investigated. No information is available about the energy spectrum of radiation defects in other A^4B^6 semiconductors.

The microscopic structure of radiation defects in A^4B^6 semiconductors continues to be one of the most complicated and unsolved problems. Further information about the nature of deep centers can be obtained by comparing the experimental data from the initial undoped, doped and electron-irradiated crystals.

Finally, the investigation of the energy spectrum of electron-irradiated doped A^4B^6 semiconductors, which was not considered in this review, is another interesting subject. The interaction of primary radiation defects and impurities may lead to the emergence of new types of defects and the corresponding deep levels in the energy spectrum of the alloys. The first publications on this subject point towards a strong interaction of the defect-formation processes upon electron irradiation and doping of $Pb_{1-x}Sn_xTe$ alloys by III group impurities[60,61] and raise hopes of a considerable modification of the energy spectrum under a combined effect of the above-mentioned factors.

This research was carried out under partial financial support from the Russian Fund for Fundamental Research.

*E-mail: skip@mig.phys.msu.su

[1]G. J. Sizoo and K. H. Onnes, Proc. Amsterdam Acad. **34**, 606 (1925).
[2]B. G. Lazarev and L. S. Kan, Zh. Éksp. Teor. Fiz. **14**, 437 (1944).
[3]N. B. Brandt, O. N. Belousova, V. P. Zlomanov *et al.*, Zh. Éksp. Teor. Fiz. **74**, 646 (1978) [Sov. Phys. JETP **47**, 340 (1978)].
[4]N. B. Brandt, Ya. G. Ponomarev, and E. P. Skipetrov, Fiz. Tverd. Tela (Leningrad) **29**, 3233 (1987) [Sov. Phys. Solid State **29**, 1856 (1987)].
[5]B. A. Akimov, L. I. Ryabova, O. B. Yatsenko, and S. M. Chudinov, Fiz. Tekh. Poluprovod. **13**, 752 (1979) [Sov. Phys. Semicond. **13**, 441 (1979)].
[6]B. A. Akimov, A. V. Dmitriev, D. R. Khokhlov, and L. I. Ryabova, Phys. Stat. Solidi (a) **137**, 9 (1993).
[7]N. B. Brandt, V. V. Dmitriev, E. A. Ladygin, and E. P. Skipetrov, Fiz. Tekh. Poluprovod. **21**, 514 (1987) [Sov. Phys. Semicond. **21**, 315 (1987)].
[8]V. V. Dmitriev and E. P. Skipetrov, Fiz. Tekh. Poluprovod. **24**, 897 (1990) [Sov. Phys. Semicond. **24**, 564 (1990)].
[9]R. Dalven, Infrared Phys. **9**, 141 (1969).
[10]G. Martinez, in *Physics of IV–VI Compounds and Alloys* (Ed. by S. Rabii), Gordon and Breach, New York (1974).
[11]J. Melngailis, J. A. Kafalas, and T. C. Harman, in *The Physics of Semimetals and Narrow-Gap Semiconductors* (Ed. by D. L. Carter and R. T. Bate), Pergamon Press, New York (1971).
[12]J. O. Dimmock, in *The Physics of Semimetals and Narrow-Gap Semiconductors* (Ed. by D. L. Carter and R. T. Bate), Pergamon Press, New York (1971).
[13]G. Martinez, Phys. Rev. B **8**, 4678 (1973).
[14]G. Nimtz and B. Schlicht, in *Narrow-Gap Semiconductors* (Ed. by R. Dornhaus, G. Nimtz and B. Schlicht), Springer-Verlag, Berlin (1983).
[15]H. T. Harper, B. A. Green, R. E. Leadon, and J. A. Naber, IEEE Trans. Nucl. Sci. **NS-21**, 30 (1974).
[16]J. A. Naber, R. E. Leadon, H. T. Harper *et al.*, in *Lattice Defects in Semiconductors*, Inst. Phys. Conf. Ser. N23, 325 (1975).
[17]B. A. Green, J. Appl. Phys. **47**, 2243 (1976).
[18]V. N. Brudnyi, A. V. Voitsekhovskii, M. A. Krivov *et al.*, Fiz. Tekh. Poluprovod. **12**, 1495 (1978) [Sov. Phys. Semicond. **12**, 885 (1978)].
[19]A. V. Voitsehovski, V. N. Broudnyi, Yu. V. Lilenko *et al.*, Solid State Communs. **31**, 105 (1979).
[20]N. J. Parada and G. W. Pratt, Phys. Rev. Lett. **22**, 180 (1969).
[21]N. J. Parada, Phys. Rev. B **3**, 2042 (1971).
[22]G. W. Pratt, J. Nonmetals, **1**, 103 (1973).
[23]L. A. Hemstreet, Phys. Rev. B **11**, 2260 (1975).
[24]L. A. Hemstreet, Phys. Rev. B **12**, 1212 (1975).
[25]B. A. Volkov and O. A. Pankratov, Dokl. Akad. Nauk SSSR **255**, 93 (1980) [Sov. Phys. Doklady **25**, 922 (1980)].
[26]B. A. Volkov and O. A. Pankratov, Zh. Éksp. Teor. Fiz. **88**, 280 (1985) [Sov. Phys. JETP **61**, 164 (1985)].
[27]O. A. Pankratov and P. P. Povarov, Fiz. Tverd. Tela (Leningrad) **30**, 880 (1988) [Sov. Phys. Solid State **30**, 508 (1988)].
[28]O. A. Pankratov and P. P. Povarov, Solid State Communs. **66**, 847 (1988)].
[29]B. B. Kovalev and E. P. Skipetrov, Fiz. Tekh. Poluprovod. **24**, 1379 (1990) [Sov. Phys. Semicond. **24**, 866 (1990)].
[30]N. B. Brandt, B. B. Kovalev, and E. P. Skipetrov, Semicond. Sci. Techn. **6**, 487 (1991).
[31]N. B. Brandt, E. P. Skipetrov, E. I. Slyn'ko *et al.*, Fiz. Tekh. Poluprovod. **24**, 51 (1990) [Sov. Phys. Semicond. **24**, 31 (1990)].
[32]N. B. Brandt, E. P. Skipetrov, and A. G. Khorosh, Fiz. Tekh. Poluprovod. **26**, 888 (1992) [Sov. Phys. Semicond. **26**, 500 (1992)].
[33]T. F. Tao, C. C. Wang, and J. W. Sunier, Appl. Phys. Lett. **20**, 235 (1972).
[34]C. C. Wang, T. F. Tao, and J. W. Sunier, J. Appl. Phys. **45**, 3981 (1974).
[35]N. B. Brandt, A. M. Gas'kov, E. A. Ladygin *et al.*, Fiz. Tekh. Poluprovod. **23**, 2034 (1989) [Sov. Phys. Semicond. **23**, 1258 (1989)].
[36]N. B. Brandt, V. P. Zlomanov, E. A. Ladygin *et al.*, Fiz. Tverd. Tela (Leningrad) **29**, 246 (1987).
[37]N. B. Brandt, V. P. Dubkov, E. P. Skipetrov, and E. A. Ladigin, Solid State Communs. **65**, 1489 (1988).
[38]N. B. Brandt, V. N. Doropei, V. P. Dubkov, and E. P. Skipetrov, Fiz. Tekh. Poluprovod. **22**, 1462 (1988) [Sov. Phys. Semicond. **22**, 925 (1988)].
[39]N. B. Brandt and E. P. Skipetrov, Semicond. Sci. Tech. **4**, 260 (1989).
[40]E. P. Skipetrov, V. P. Dubkov, and B. B. Kovalev, Semicond. Sci. Tech. **4**, 831 (1989).
[41]N. B. Brandt and E. P. Skipetrov, High Pressure Research **3**, 9 (1990).
[42]E. P. Skipetrov, in *Structure and Properties of* $A^{IV}B^{VI}$ *Compounds* (ed. by A. N. Kovalev) [in Russian], Metallurgiya, Moscow (1990).
[43]Ya. G. Ponomarev and E. P. Skipetrov, in *Structure and Properties of* $A^{IV}B^{VI}$ *Compounds* (ed. by A. N. Kovalev) [in Russian], Metallurgiya, Moscow (1990).
[44]N. B. Brandt, V. P. Dubkov, G. V. Ivanova *et al.*, Vest. Mosk. Univ., Ser. 3, Fizika. Astronomia **28**, 96 (1987).
[45]N. B. Brandt, V. P. Dubkov, V. P. Zlomanov *et al.*, Fiz. Tekh. Poluprovod. **21**, 2136 (1987) [Sov. Phys. Semicond. **21**, 1297 (1987)].
[46]E. P. Skipetrov, V. P. Dubkov, A. M. Musalitin, and I. N. Podsekalov, Fiz. Tekh. Poluprovod. **22**, 1785 (1988) [Sov. Phys. Semicond. **22**, 1129 (1988)].
[47]E. P. Skipetrov, Solid State Communs. **69**, 1053 (1989).
[48]E. P. Skipetrov, V. P. Dubkov, V. P. Zlomanov *et al.*, Izv. Akad. Nauk SSSR. Neorg. Mater. **25**, 737 (1989).
[49]V. P. Dubkov and E. P. Skipetrov, Fiz. Tekh. Poluprovod. **24**, 104 (1990) [Sov. Phys. Semicond. **24**, 63 (1990)].
[50]N. B. Brandt, B. B. Kovalev, and E. P. Skipetrov, Fiz. Tekh. Vysok. Davl. No. 12, 5 (1992).
[51]E. P. Skipetrov and B. B. Kovalev, Neorg. Mater. **28**, 2322 (1992).
[52]B. A. Volkov, I. V. Kucherenko, V. N. Moiseenko, and A. P. Shotov, Pis'ma Zh. Éksp. Teor. Fiz. **27**, 396 (1978) [JETP Lett. **27**, 371 (1978)].
[53]N. B. Brandt, Ya. G. Ponomarev, and E. P. Skipetrov, Fiz. Tekh. Poluprovod. **17**, 645 (1983) [Sov. Phys. Semicond. **17**, 403 (1983)].
[54]N. B. Brandt, B. B. Kovalev, and E. P. Skipetrov, in *Proc. IV Int. Conf. "High Pressure in Semiconductor Physics"*, Thessaloniki, Greece (1990).
[55]B. B. Kovalev and E. P. Skipetrov, in *Proc. of the VIII All-Union Symp. on Narrow-Gap Semiconductors and Semimetals*, L'vov (1991).
[56]B. A. Akimov, R. S. Wadhwa, and S. M. Chudinov, Fiz. Tekh. Poluprovod. **12**, 1927 (1978) [Sov. Phys. Semicond. **12**, 1146 (1978)].
[57]E. P. Skipetrov, A. N. Nekrasova, D. V. Pelekhov, and V. I. Sidorov, Neorg. Mater. **28**, 2372 (1992).

[58]N. B. Brandt, E. P. Skipetrov, A. N. Nekrasova, and A. V. Ryazanov, in *Abstracts of Papers to Joint XV AIRAPT and XXXIII EHPRG Intern. Conf.*, Warsaw, Poland (1995).

[59]B. A. Akimov, R. S. Wadhwa, V. P. Zlomanov *et al.*, Fiz. Tekh. Poluprovod. **11**, 1077 (1977)[Sov. Phys. Semicond. **11**, 637 (1977)].

[60]E. P. Skipetrov, A. N. Nekrasova, D. V. Pelekhov *et al.*, Fiz. Tekh. Poluprovod. **28**, 1626 (1994) [Sov. Phys. Semicond. **28**, 906 (1994)].

[61]E. P. Skipetrov, Fiz. Tekh. Poluprovod. **29**, 1416 (1995) [Sov. Phys. Semicond. **29**, 735 (1995)].

Translated by R. S. Wadhwa